Three-Dimensional Characterization of Ice Layers for Cryogenic Targets at LLE

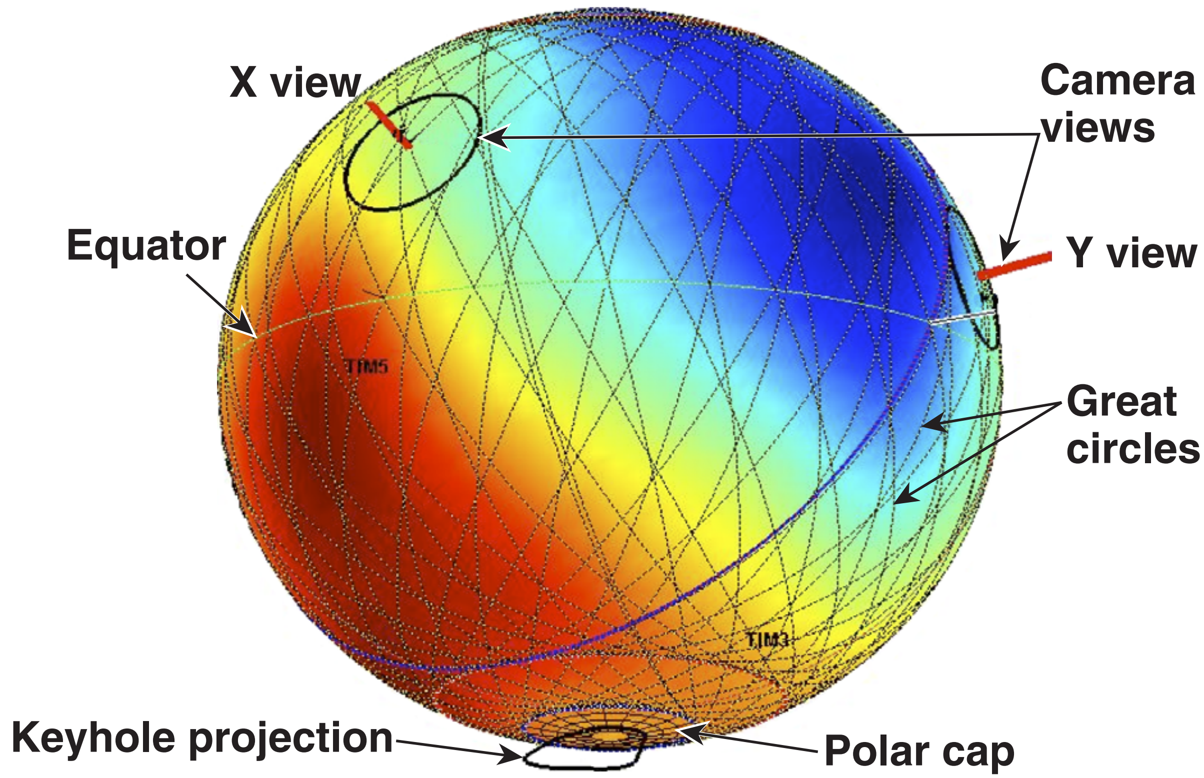

D. H. Edgell
University of Rochester
Laboratory for Laser Energetics

46th Annual Meeting of the
American Physical Society
Division of Plasma Physics
Savannah, GA
15–19 November 2004

Summary

Optimization of layering geometry will be required to eliminate ice layer nonuniformities

- 3-D target characterization is standard operating procedure for OMEGA cryogenic targets.
- The D_2 ice index of refraction has been identified as ~1.15.
- Relayering was observed upon rotation of target inside the layering sphere.
  - time constants (~ 15 to 25 min near triple point)
- Target rotation and relayering studies show ice layer roughness dominated by external nonuniformities in the layering and heating geometry.

Collaborators

W. Seka, R. S. Craxton, L. Elasky, D. R. Harding,
R. L. Keck, M. Pandina, and M. D. Wittman

Laboratory for Laser Energetics
University of Rochester

A. Warrick

Lawrence Livermore National Laboratory

T. Brown

Institute of Optics
University of Rochester

M. Alexander

Northeastern University

Shadowgraphic Analysis

Reflection and refraction due to the ice layer produces characteristic rings in shadowgraphs

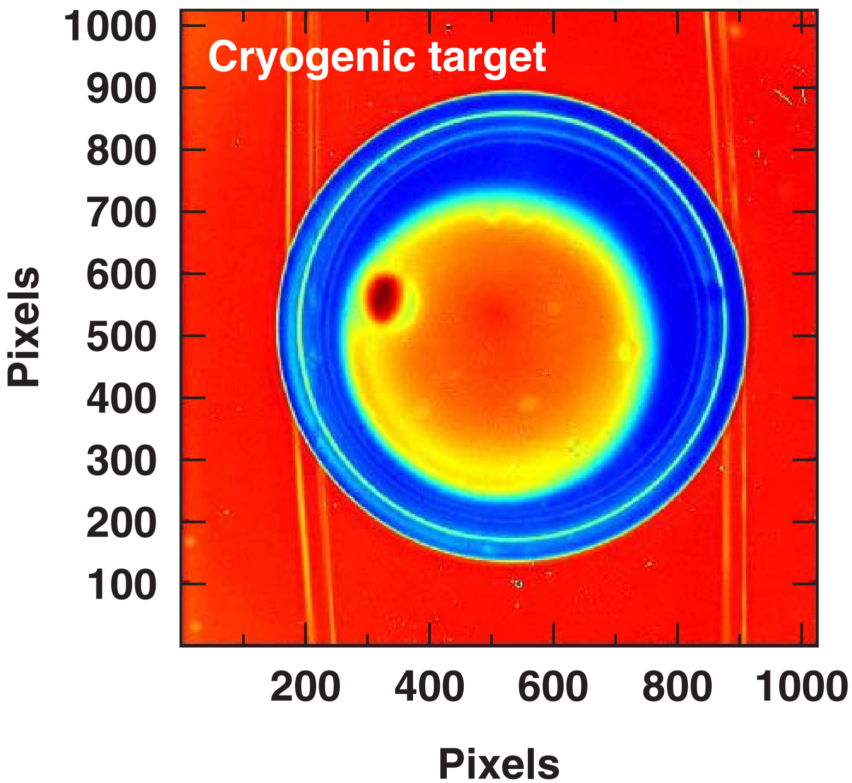

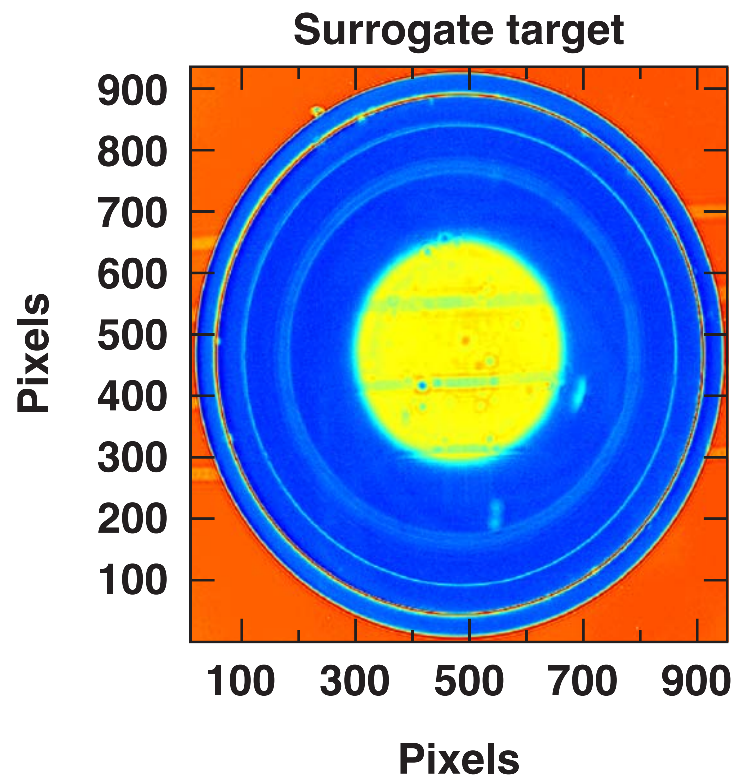

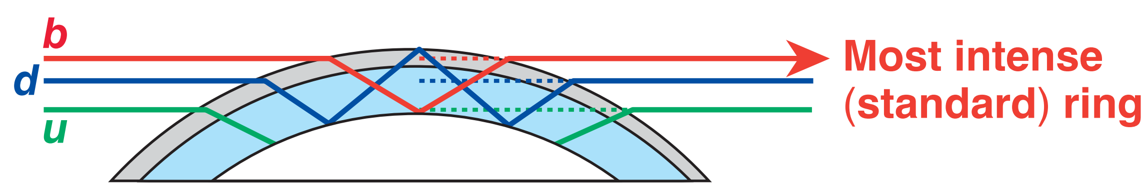

Ring positions are determined by ice thickness, surface tilt, and index of refraction.

E13425

Shadowgraphs are unwrapped around the target center to measure the Fourier modes of the rings and target surface

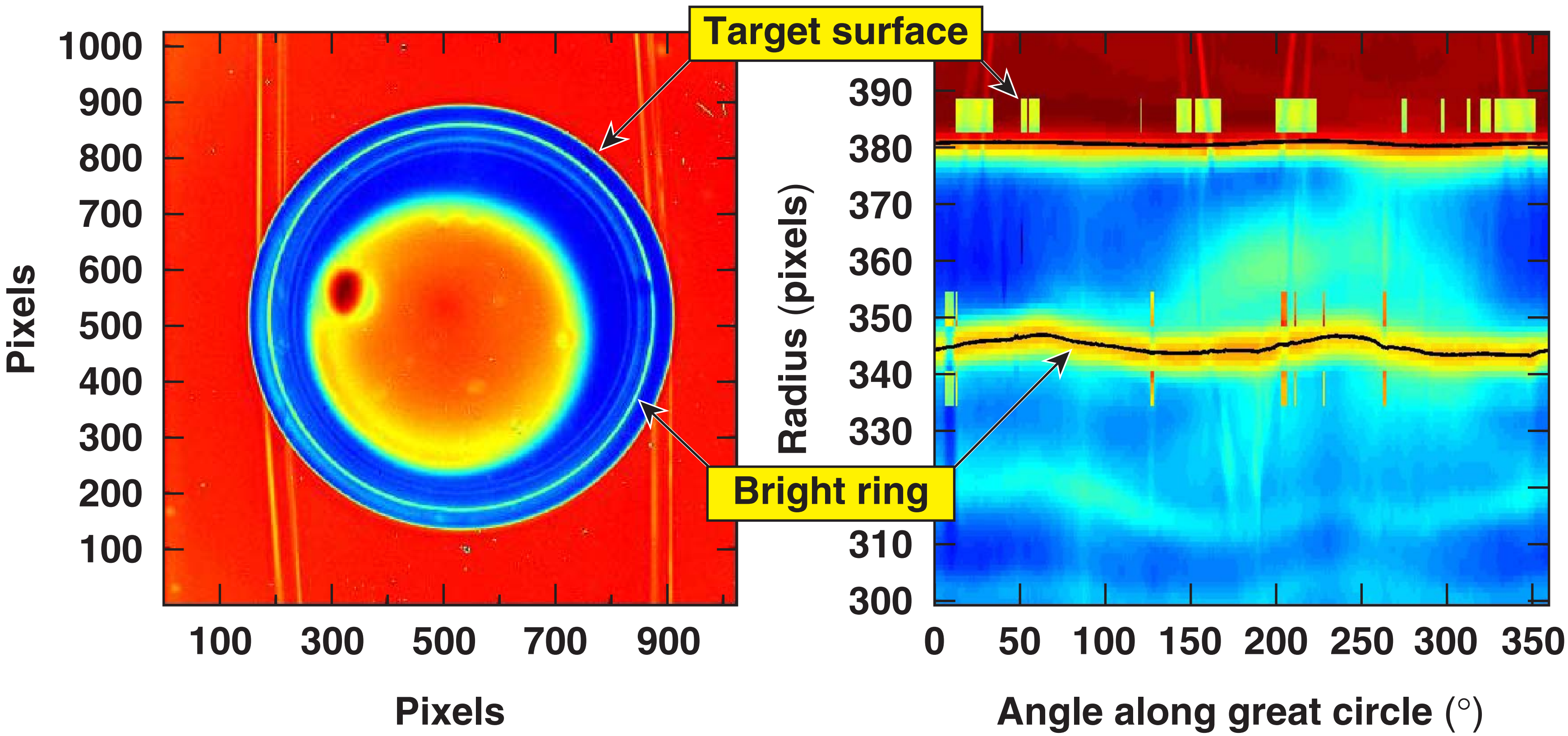

Cryo-2042-314
2y16764 s6

Unwrapped image intensity along radial lines was analyzed to determine R(θ), ring/surface radius versus polar angle.

E13426

Shadowgraphs are unwrapped around the target center to determine Fourier modes of the rings and target surface

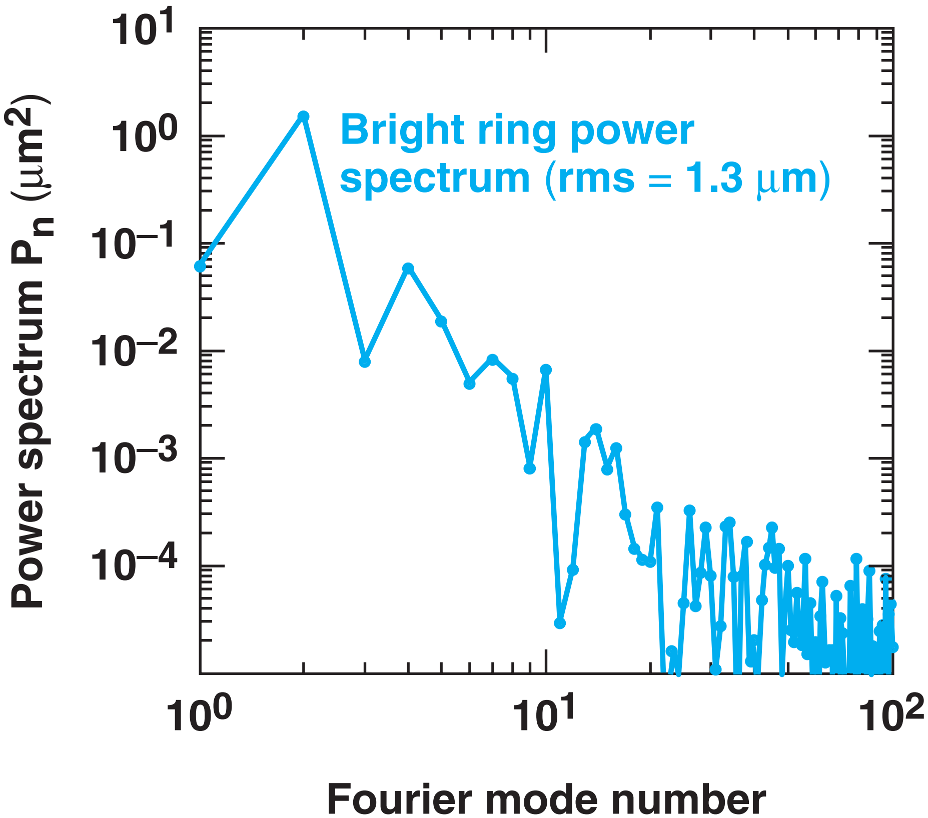

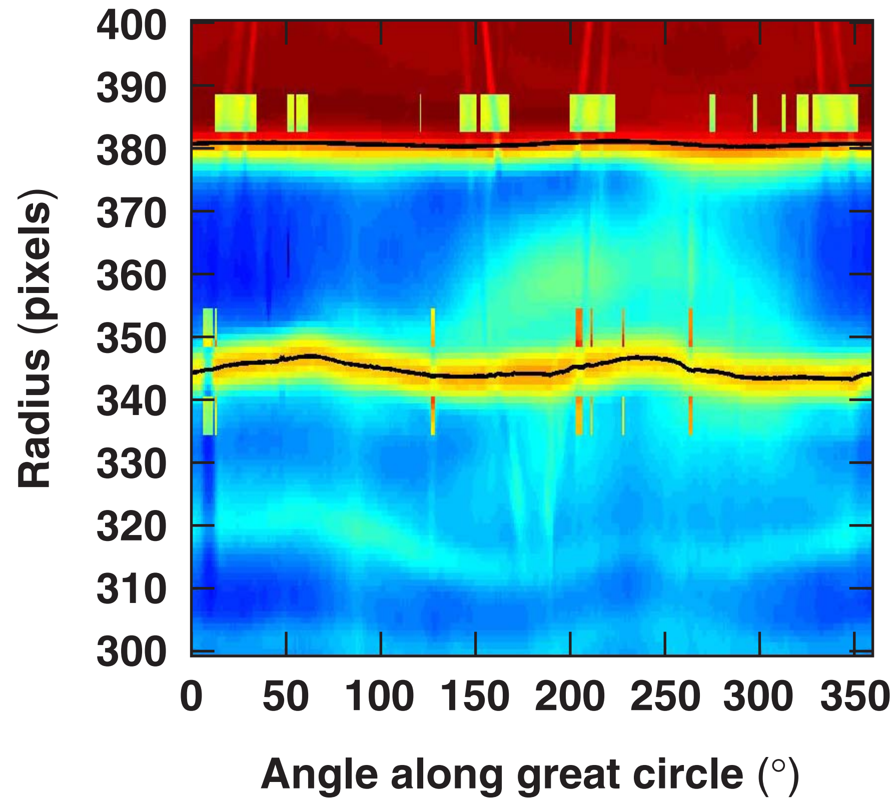

Cryo-2042-314
2y16764 s6

R(θ) analyzed to get Fourier power spectrum, P_n

E13433

3-D Ice Layer Characterization

Accurate 3-D reconstructions for implosion simulations require multiple views

15 μm offset, 4.1 μm ice rms

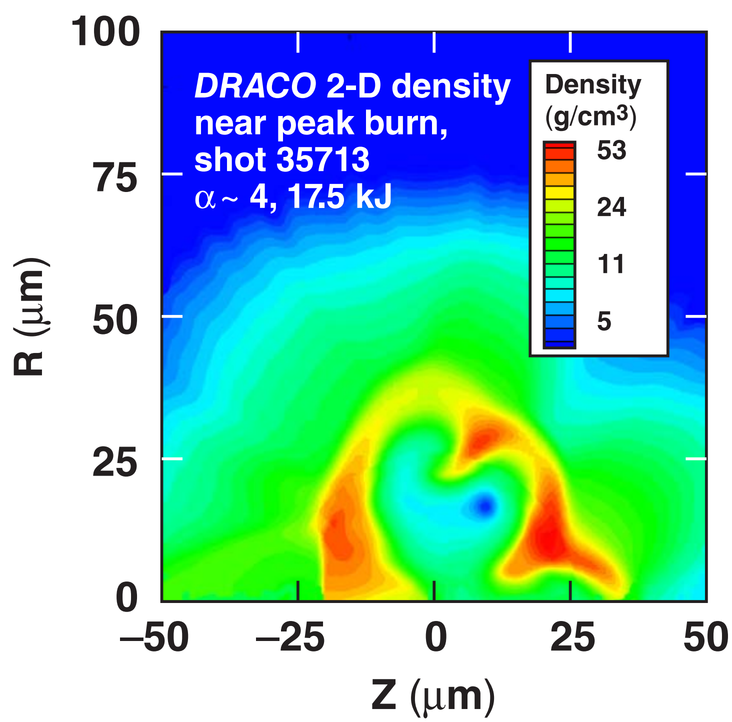

GENERAL ATOMICS

(Courtesy of R. Stephens)

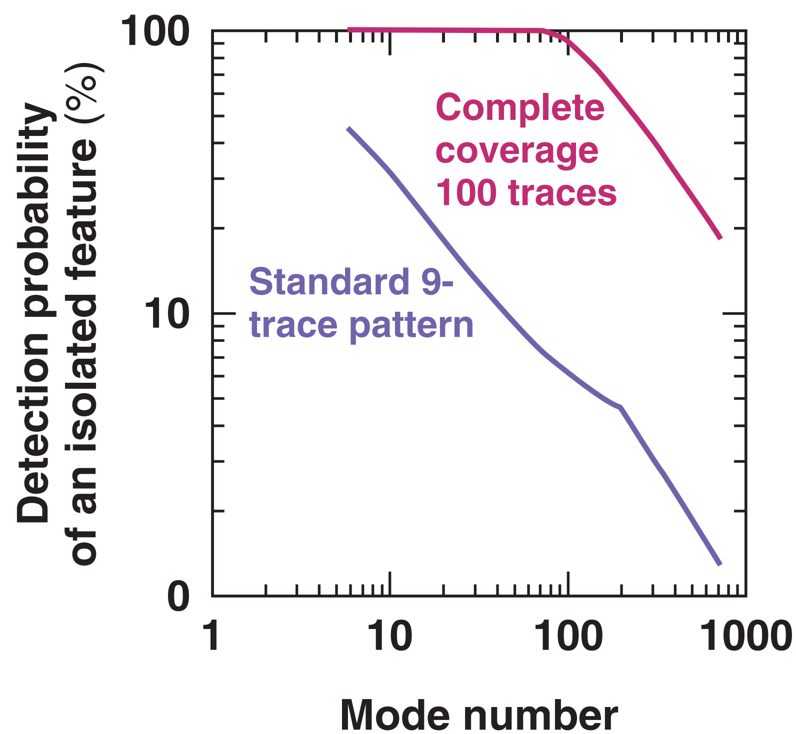

E12255e

Low-order Legendre modes are determined by a least-squares fit to spherical harmonics $Y_{\ell m}$

$$P_\ell = \sum_{m=-\ell}^{\ell} A^2_{\ell m}$$

- Great circle postitions are mapped onto a sphere.

- **The maximum ℓ-mode is limited to $\ell \lesssim 8$ to 10 by the polar caps and spacing of the great circles.**

$Y_{\ell m}$ reconstruction for $\ell_{max} = 9$
(all ℓ's and m's up to $\ell = 9$)

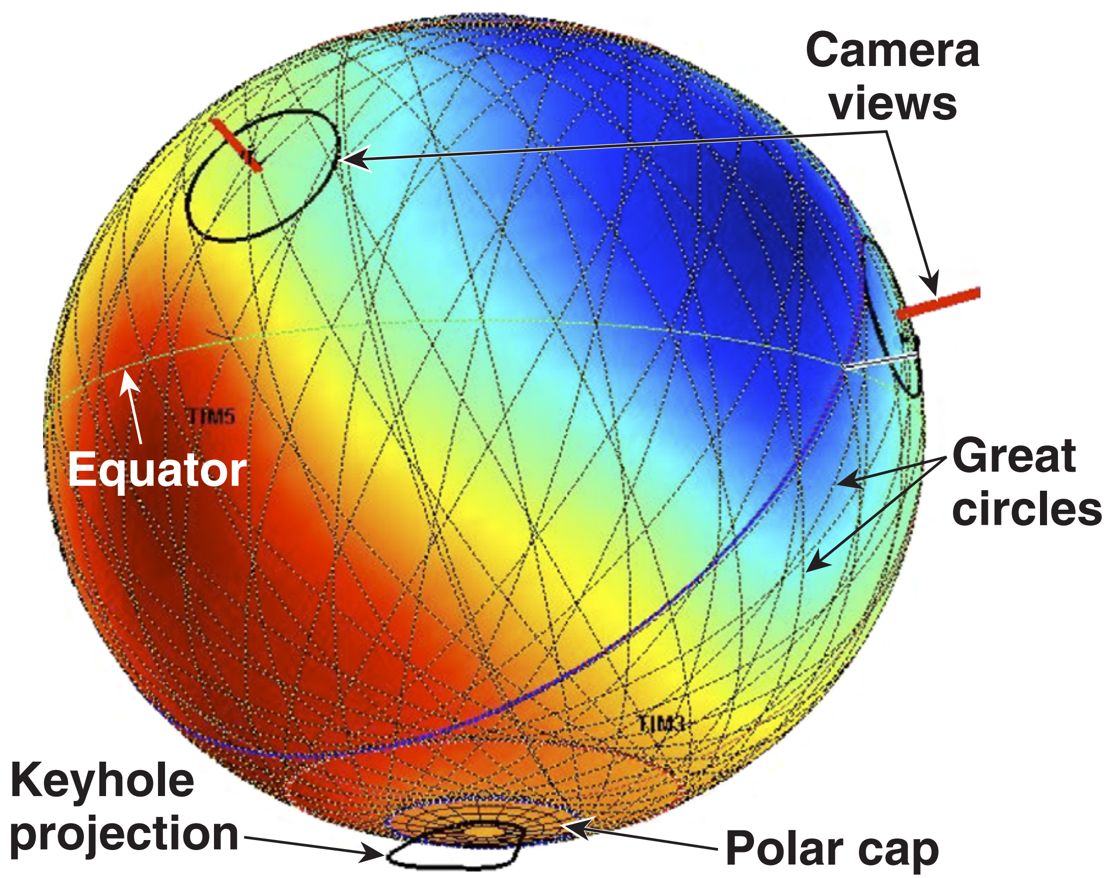

E13436

Higher-order Legendre modes are determined by a mapping from the average Fourier components*

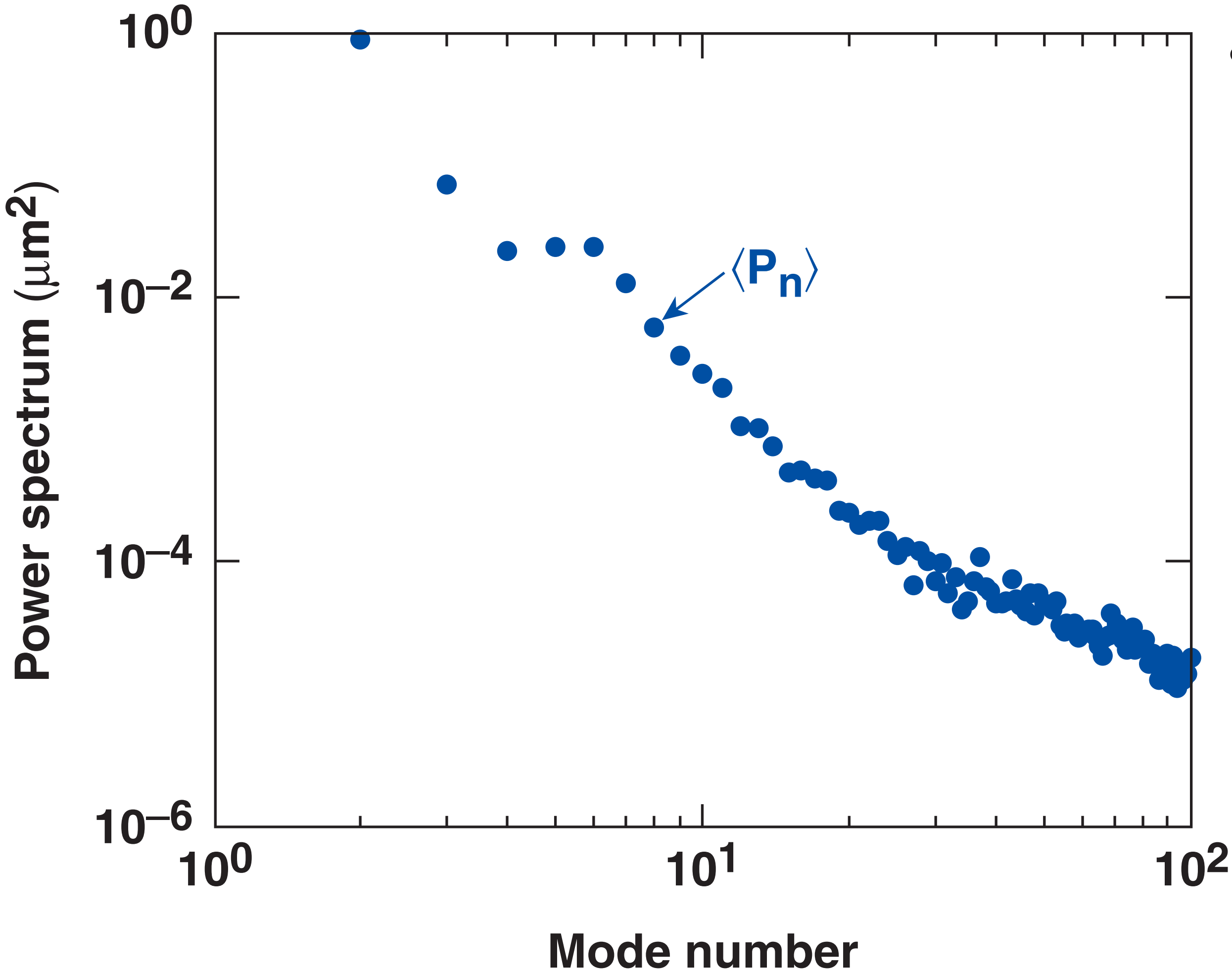

- $\langle P_n \rangle$ 2-D Fourier components averaged over many great circles.

E13434a

*S. Pollaine and S. Hatchett, Nucl. Fusion 44, 117 (2004).

Higher-order Legendre modes are determined by a mapping from the average Fourier components*

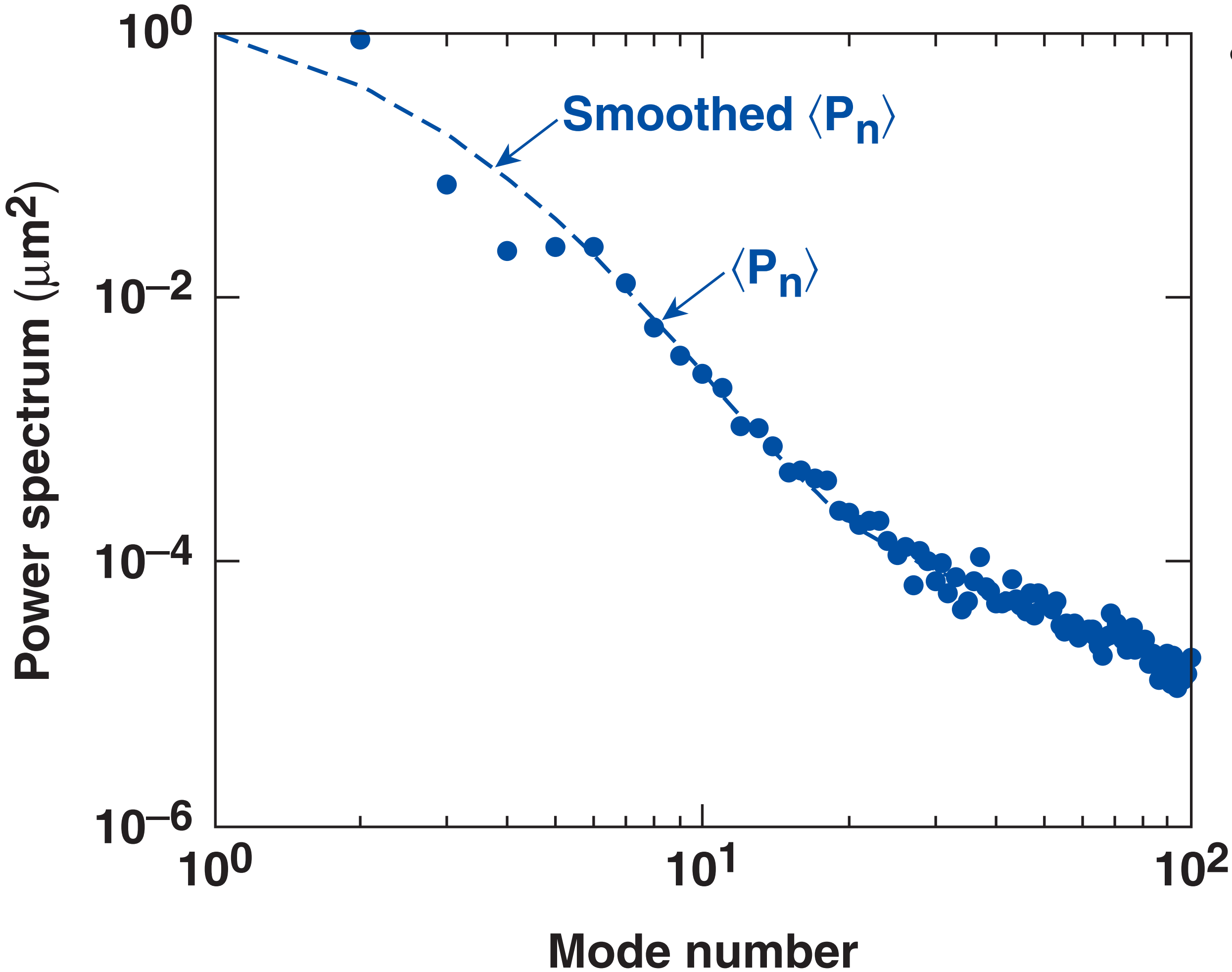

- $\langle P_n \rangle$ smoothed to improve behavior of mapping.

*S. Pollaine and S. Hatchett, Nucl. Fusion 44, 117 (2004).

E13434b

Higher-order Legendre modes are determined by a mapping from the average Fourier components*

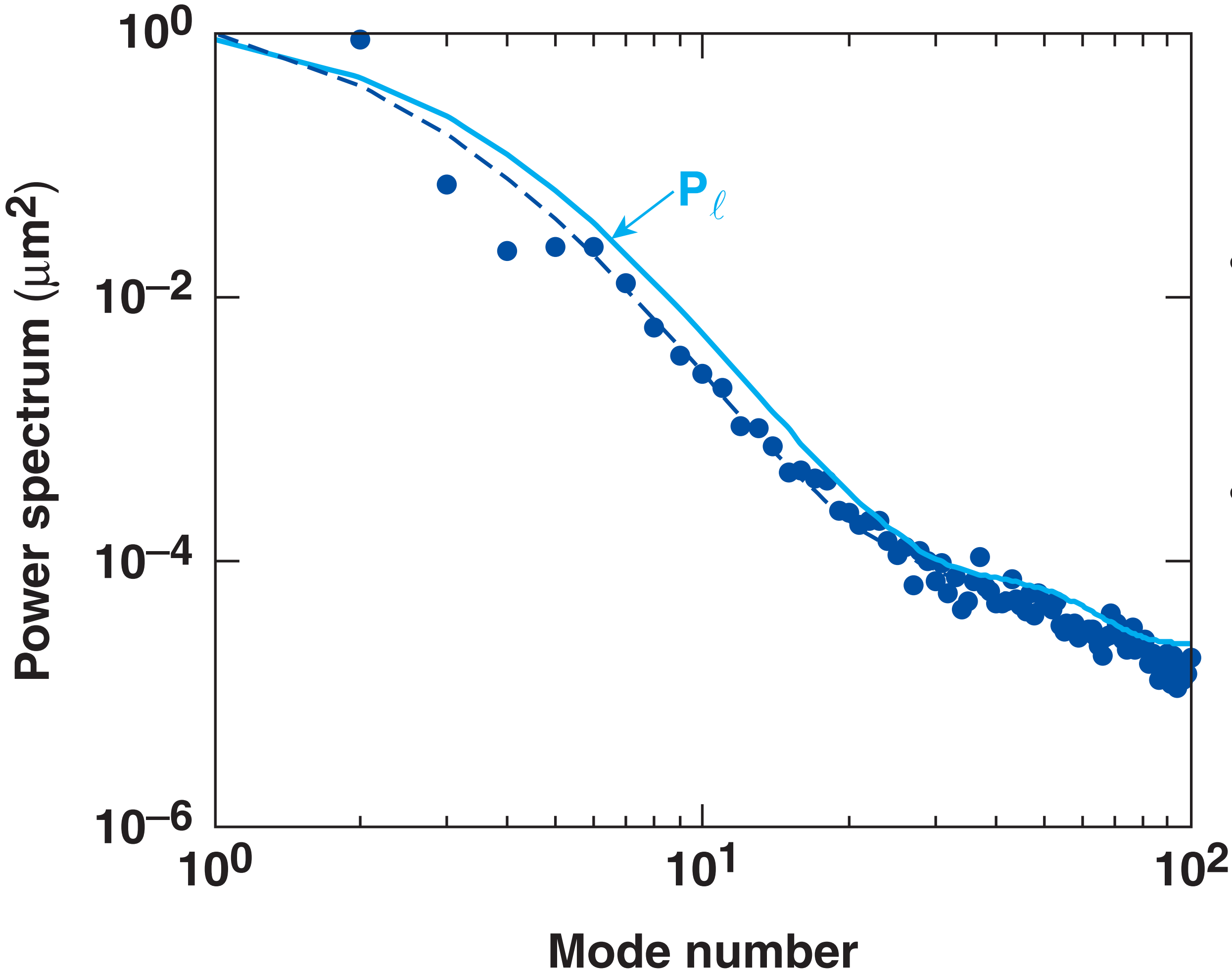

$$P_\ell = \sum_{n=\ell}^{\infty} a_{\ell n} \langle P_n \rangle$$

- Average Fourier components $\langle P_n \rangle$ mapped* to Legendre modes P_ℓ.
- Assumes isotropic distribution of perturbations.

*S. Pollaine and S. Hatchett, Nucl. Fusion 44, 117 (2004).

E13434c

Higher-order Legendre modes are determined by a mapping from the average Fourier components*

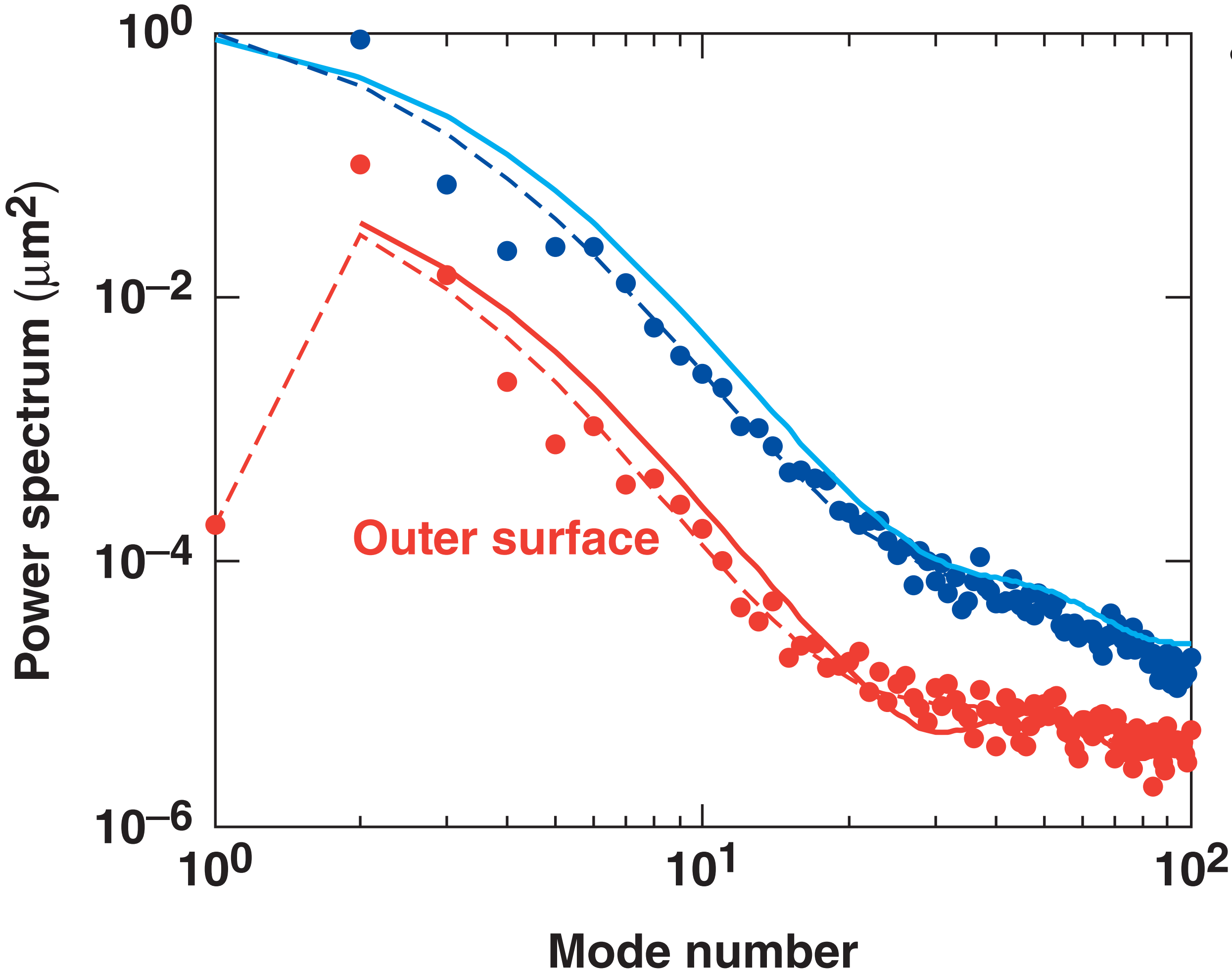

- Same procedure is applied to get outer surface of power spectrum.

E13434d

*S. Pollaine and S. Hatchett, Nucl. Fusion 44, 117 (2004).

Multiple views allow some bright ring structures to be uniquely related to target surface features

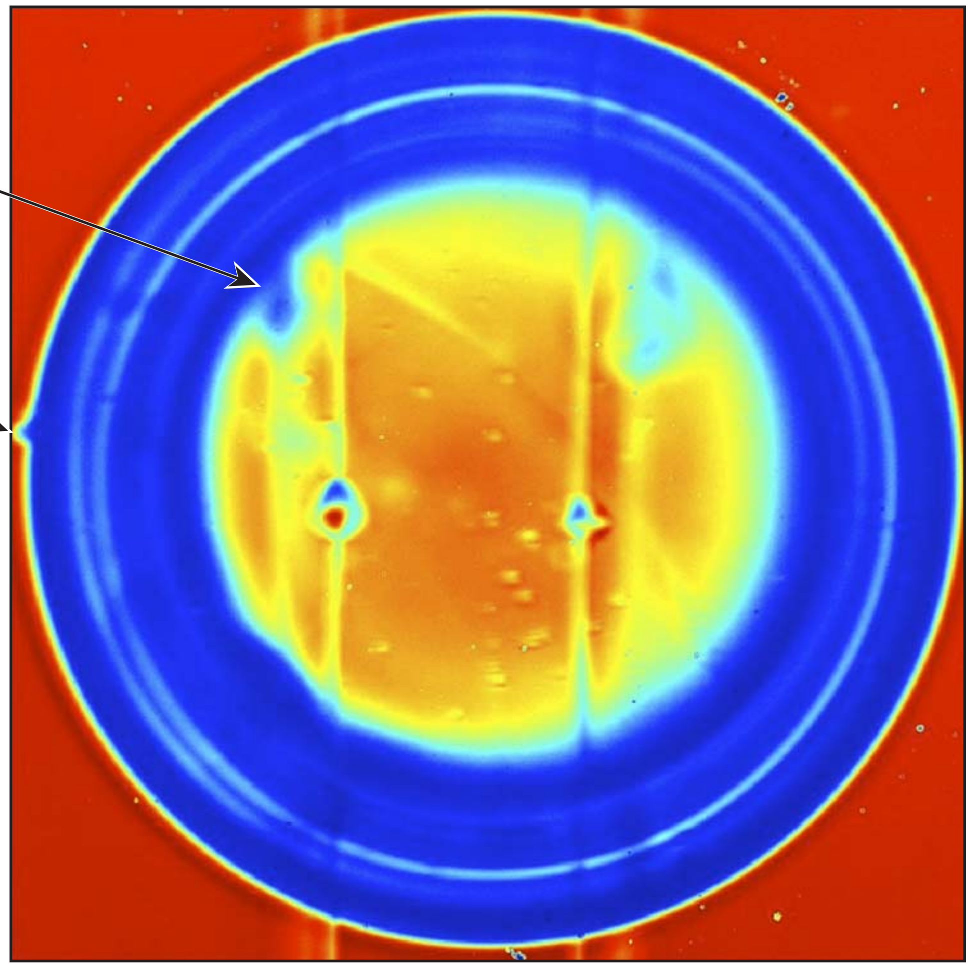

$\theta_{MCTC} = 115^{\circ}$

Multiple views allow some bright ring structures to be uniquely related to target surface features

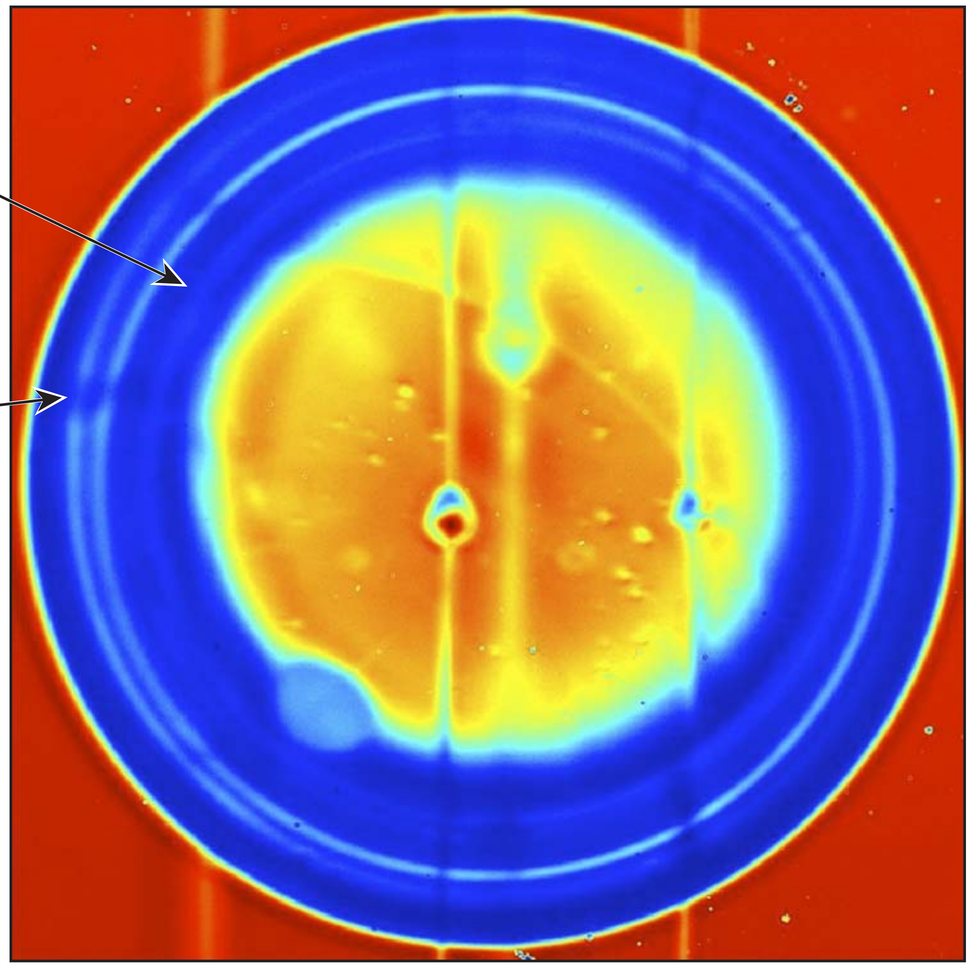

$\theta_{MCTC} = 130^\circ$

E13520a

CRYO-2038-015TAIL

Multiple views allow some bright ring structures to be uniquely related to target surface features

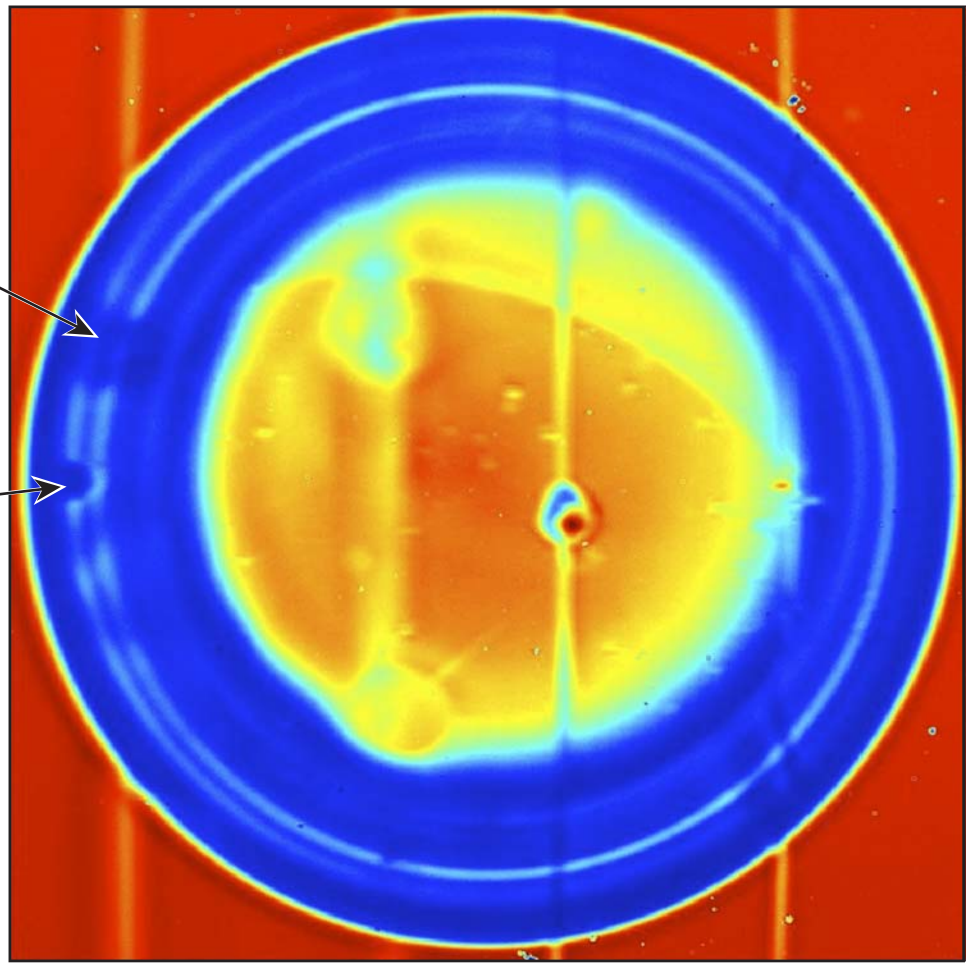

$\theta_{MCTC} = 145^{\circ}$

These ring structures are due to surface features and should not be included in ice roughness analysis.

CRYO-2038-015TAIL

Multiple views allow some some ice nonuniformities to be uniquely identified

Convex feature on inner ice surface closest to camera

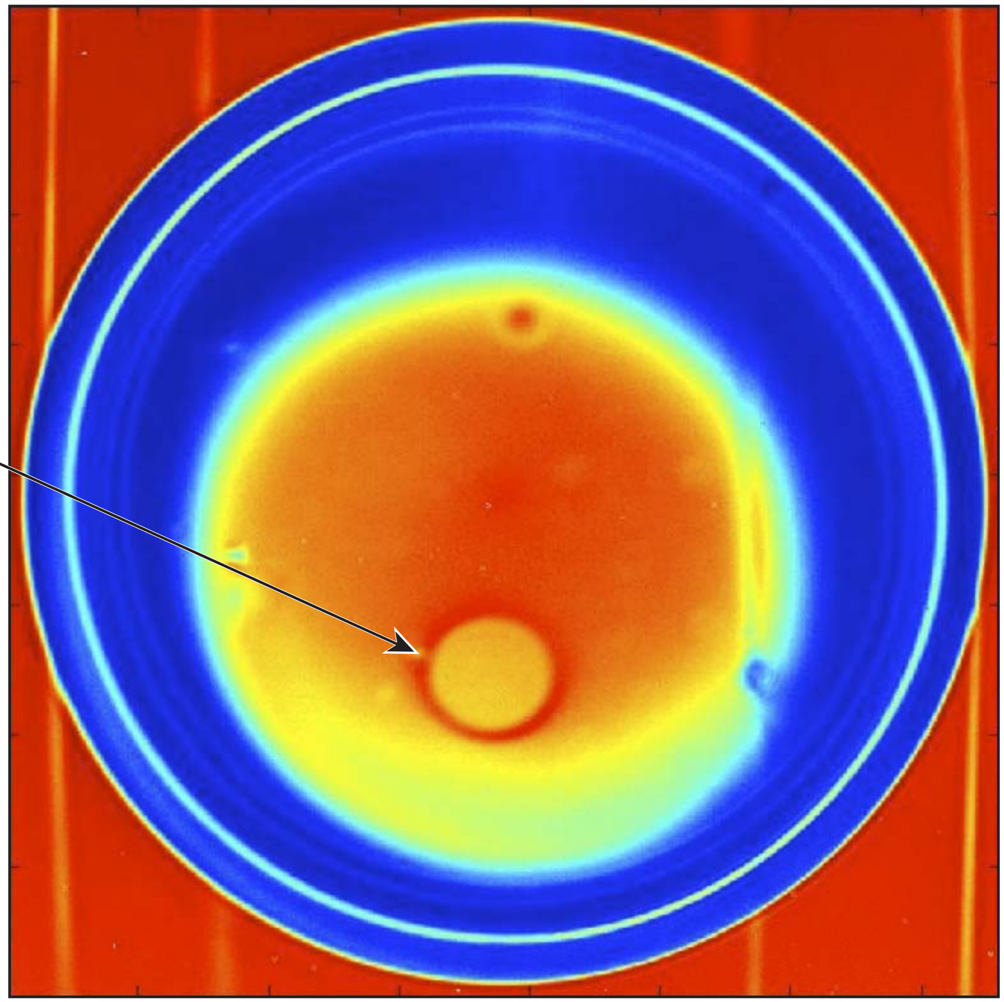

E13524

Multiple views allow some some ice nonuniformities to be uniquely identified

Convex feature on inner ice surface closest to camera

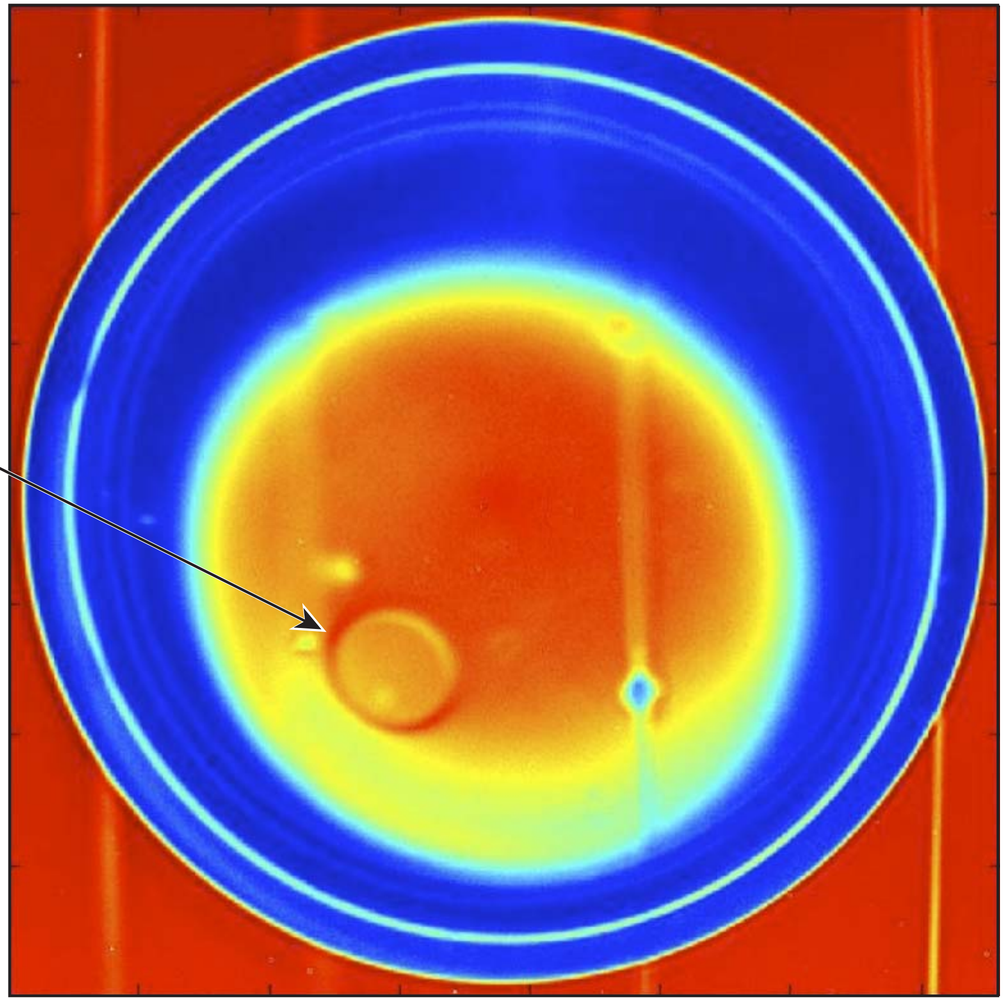

E13524a

Multiple views allow some some ice nonuniformities to be uniquely identified

Convex feature on inner ice surface closest to camera

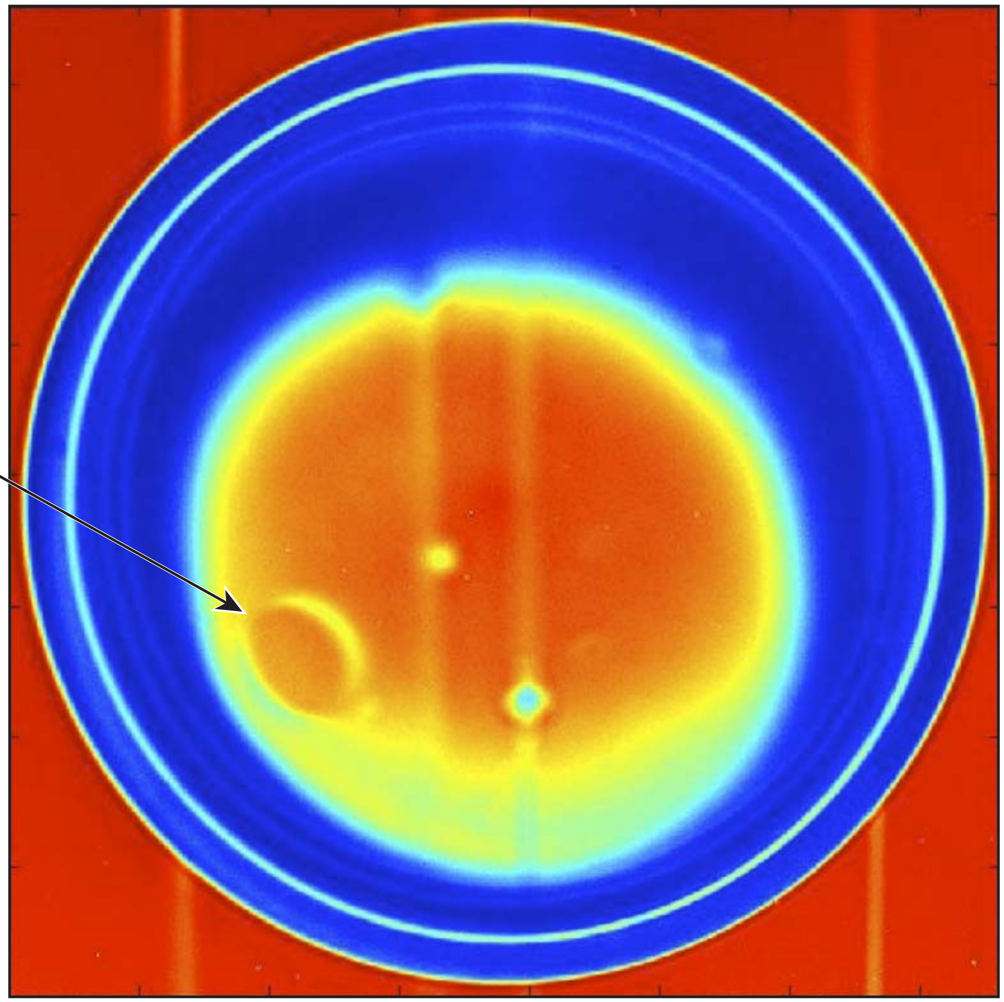

E13524b

Multiple views allow some some ice nonuniformities to be uniquely identified

Convex feature on inner ice surface closest to camera

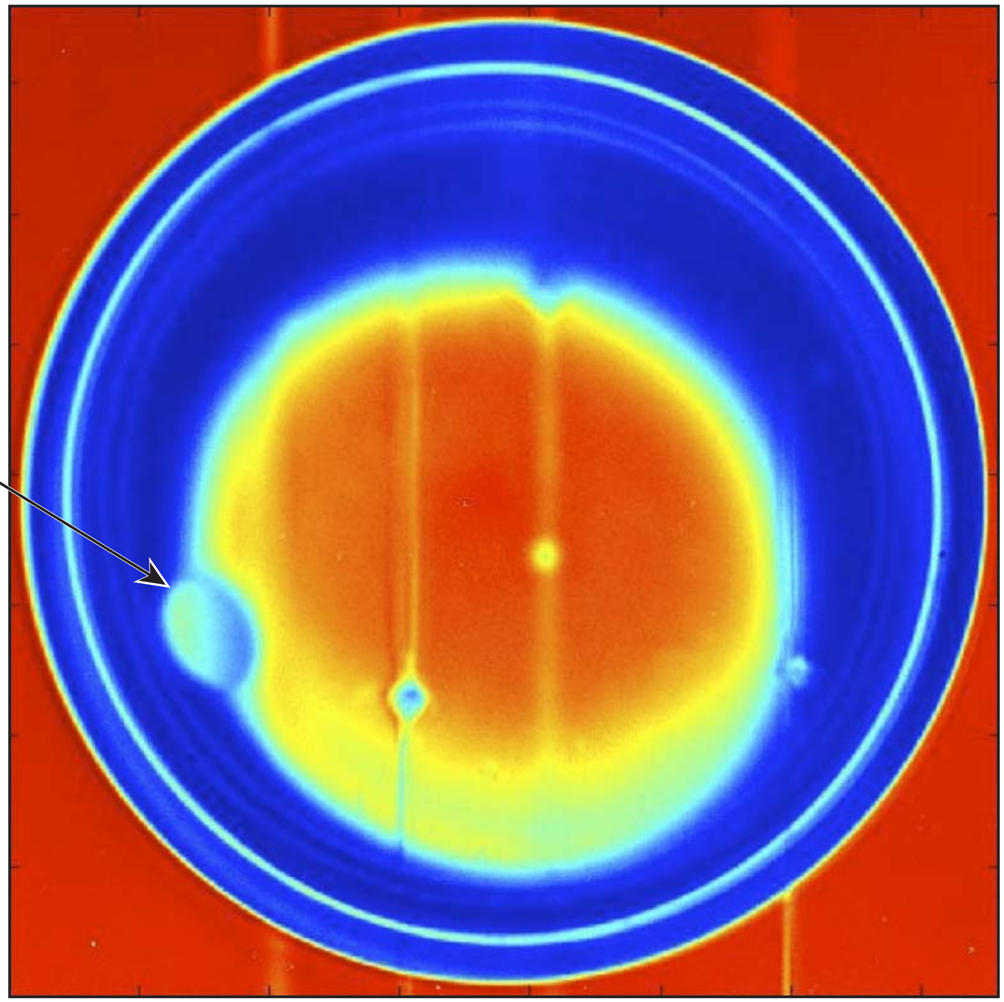

Multiple views allow some some ice nonuniformities to be uniquely identified

Convex feature on inner ice surface closest to camera

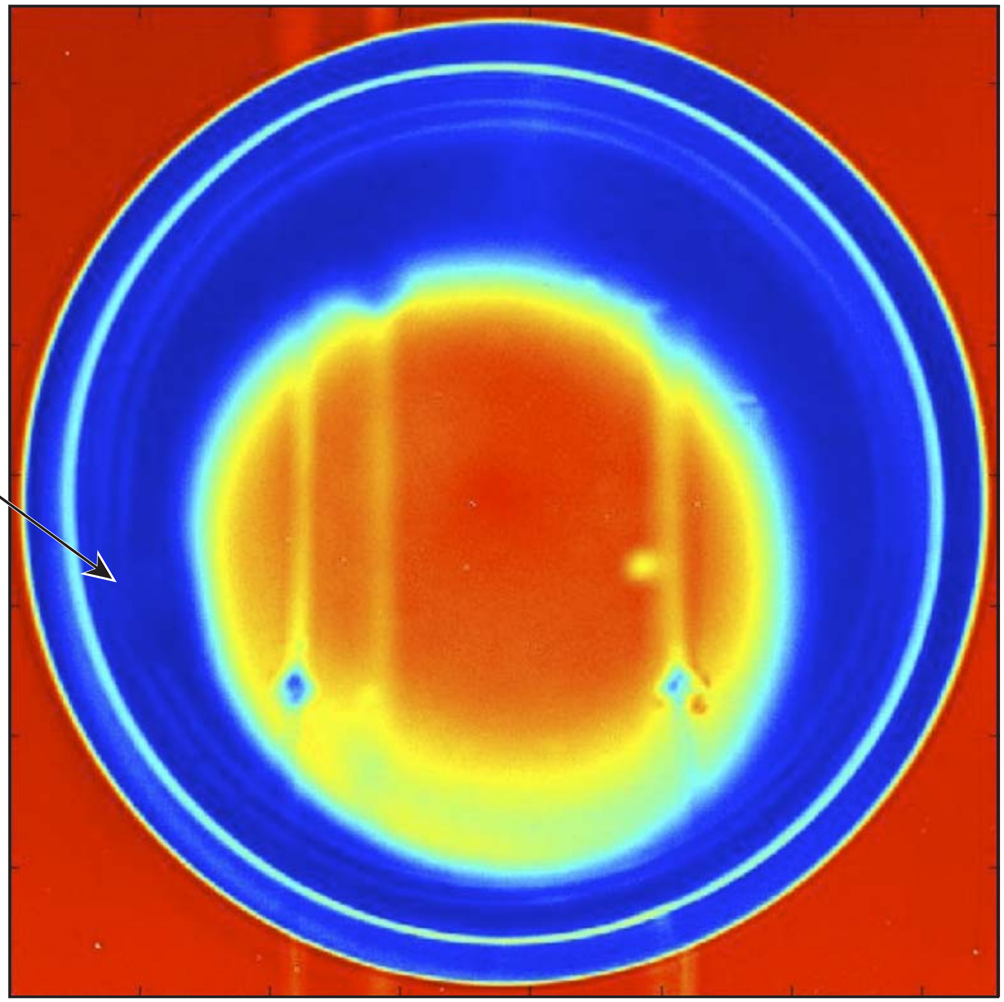

E13524d

Multiple views allow some some ice nonuniformities to be uniquely identified

Convex feature on inner ice surface closest to camera

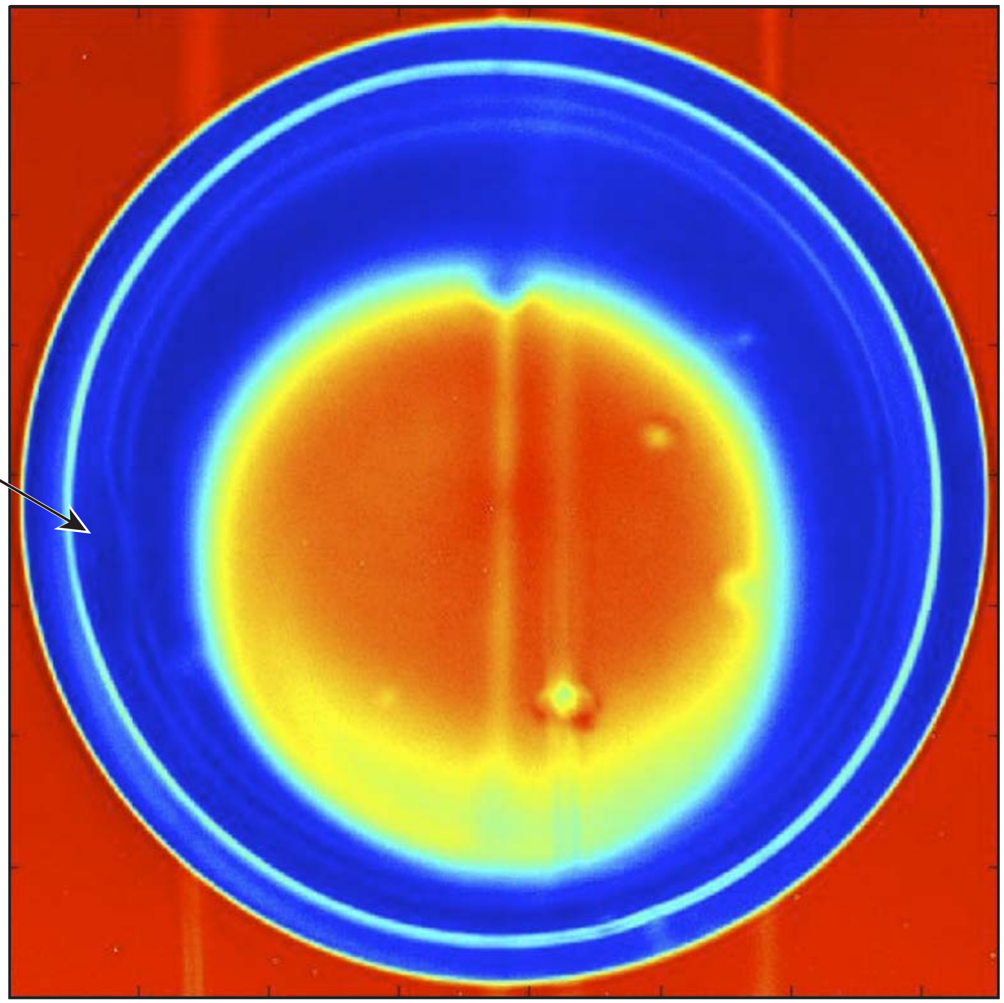

E13524e

Multiple views allow some some ice nonuniformities to be uniquely identified

Convex feature on inner ice surface closest to camera

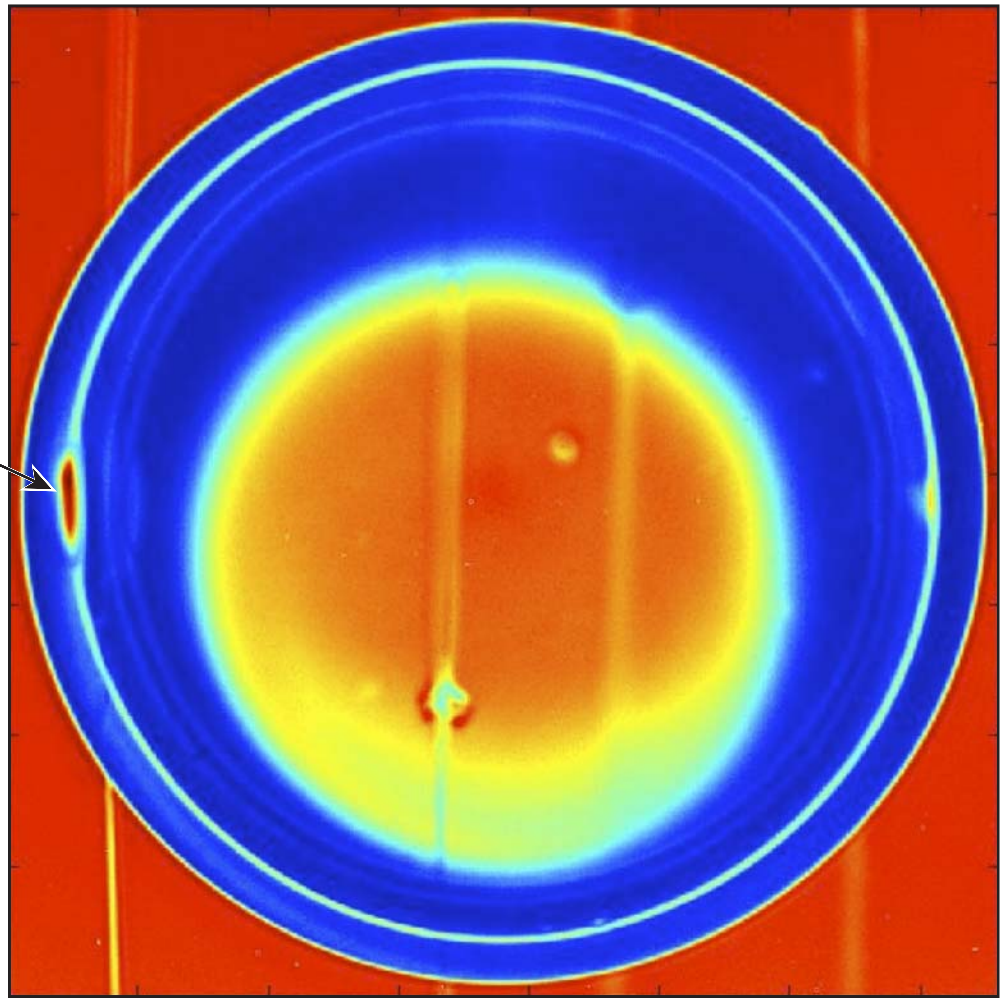

E13524f

Significant relayering occurs during a slow rotation characterization followed by a return to normal

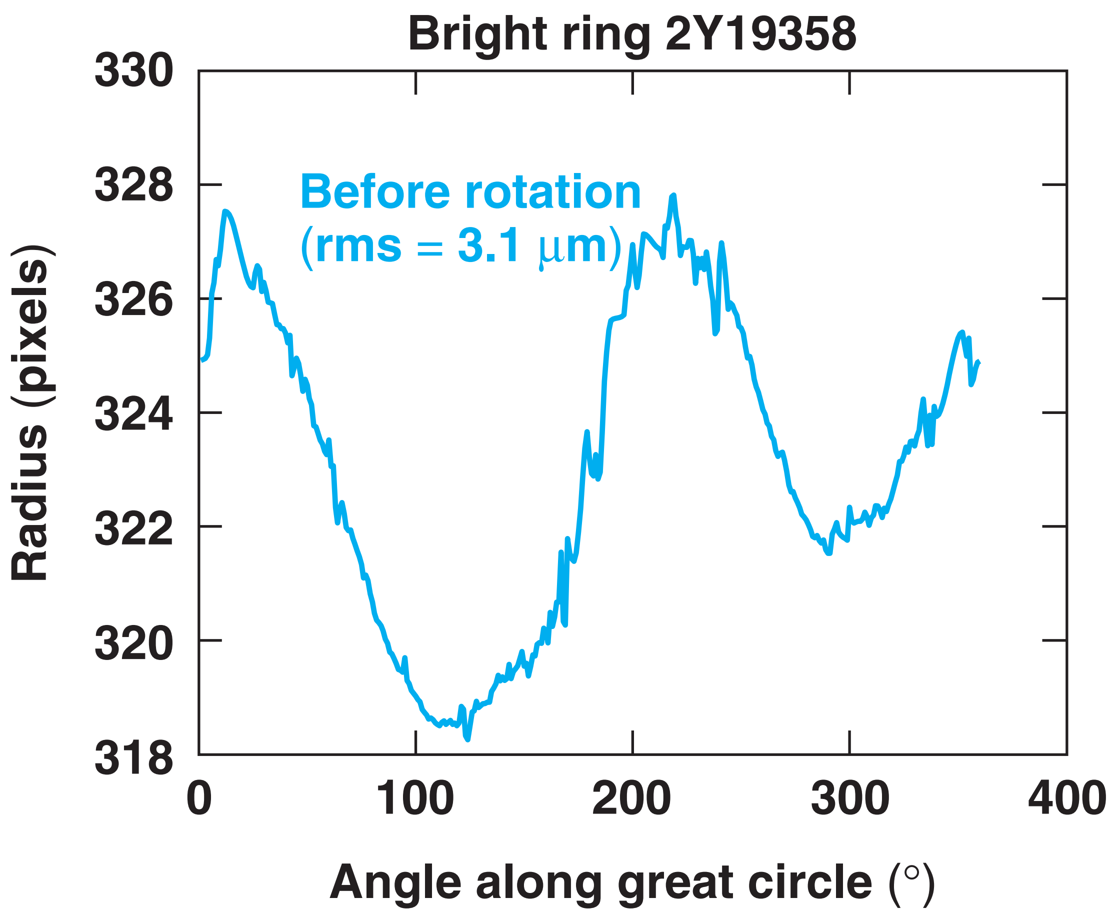

We have observed consistently different ring structures at the same viewing angle before and after a 40-min set of target rotations → relayering during rotation of the target.

E13437a

Significant relayering occurs during a slow rotation characterization followed by a return to normal

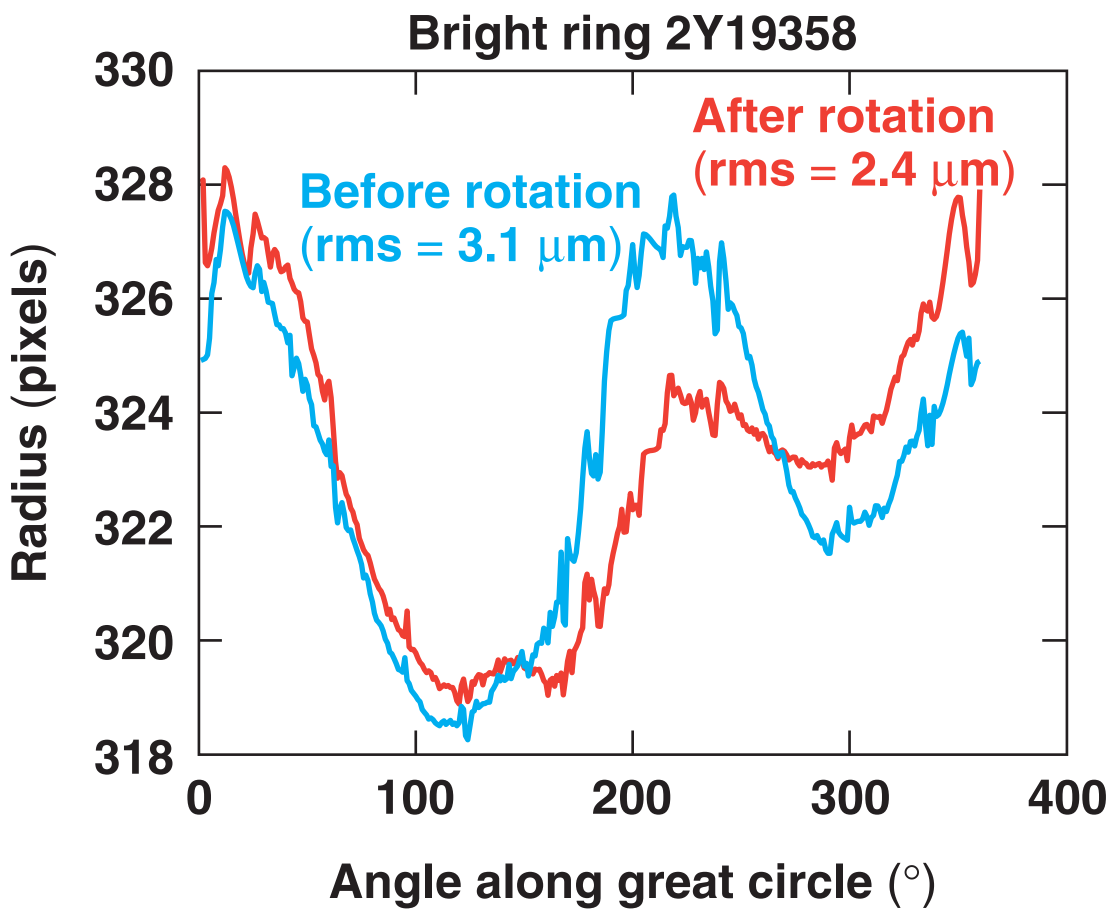

We have observed consistently different ring structures at the same viewing angle before and after a 40-min set of target rotations → relayering during rotation of the target.

E13437b

Significant relayering occurs during a slow rotation characterization followed by a return to normal

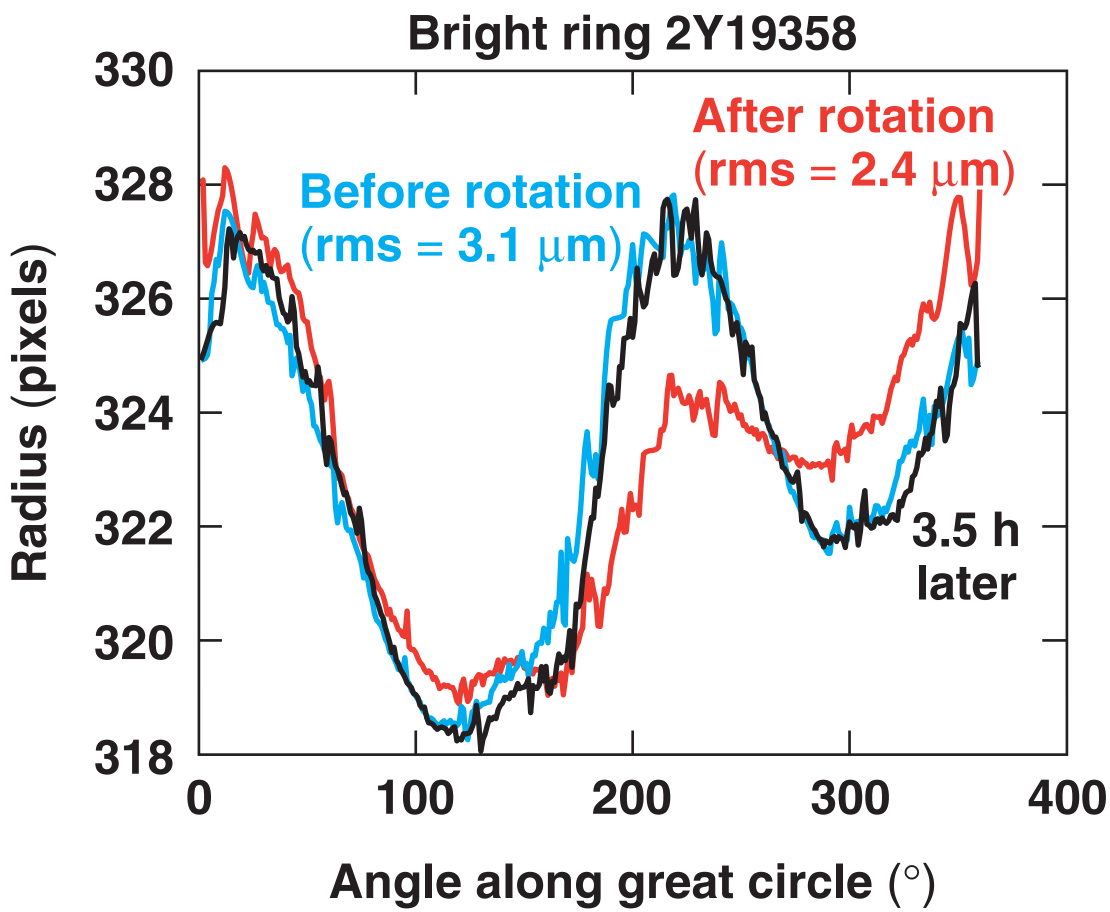

We have observed consistently different ring structures at the same viewing angle before and after a 40-min set of target rotations → relayering during rotation of the target.

E13437

Relayering occurs with a 14 to 24 min time constant after a 180° rotation

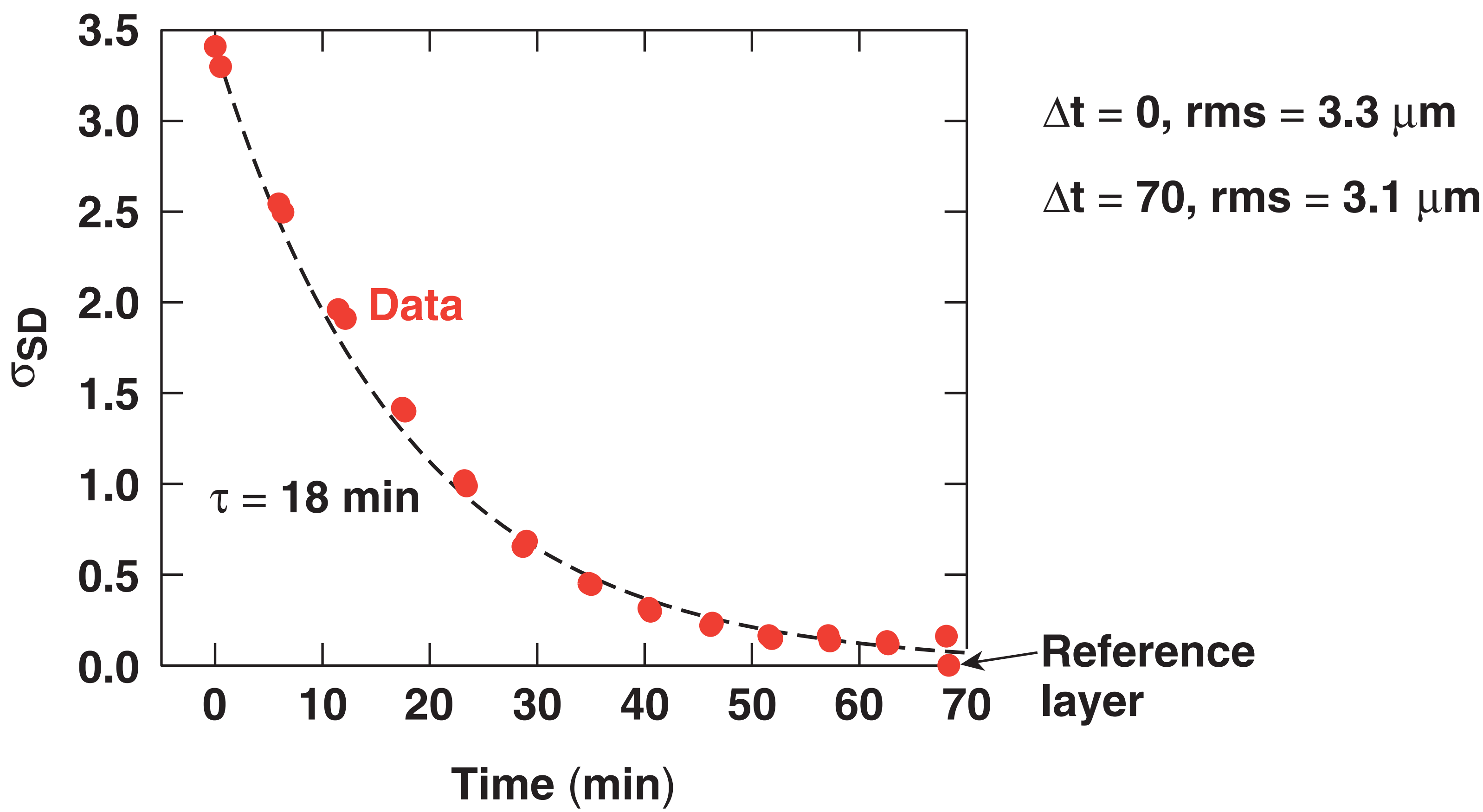

The standard deviation of difference between bright ring versus reference ring (taken at 70 min) shows a smooth relaxation to "steady state."

E13439

Reliable 3-D characterization is maintained by fast "fan" rotation to the imaging angle then back to home

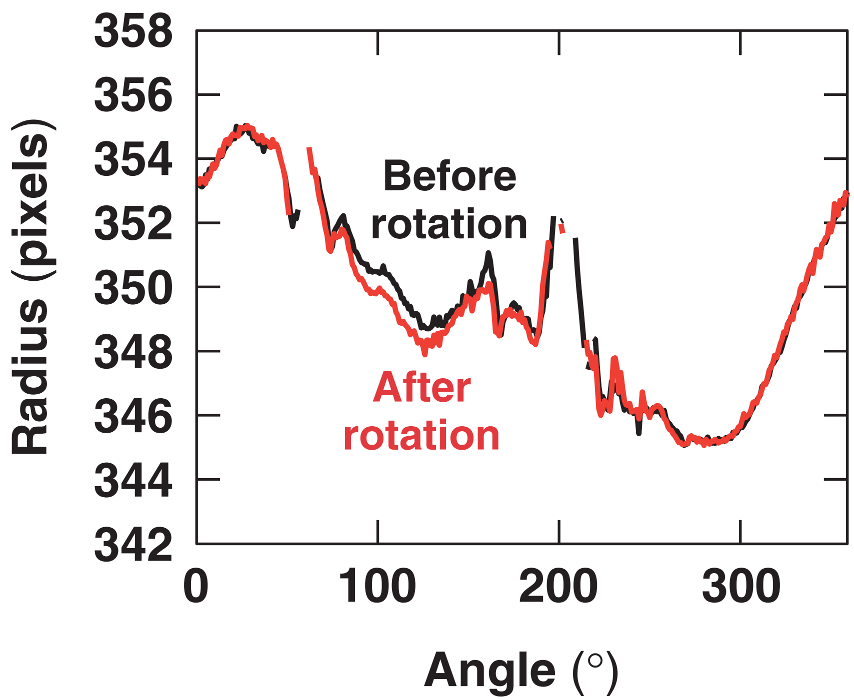

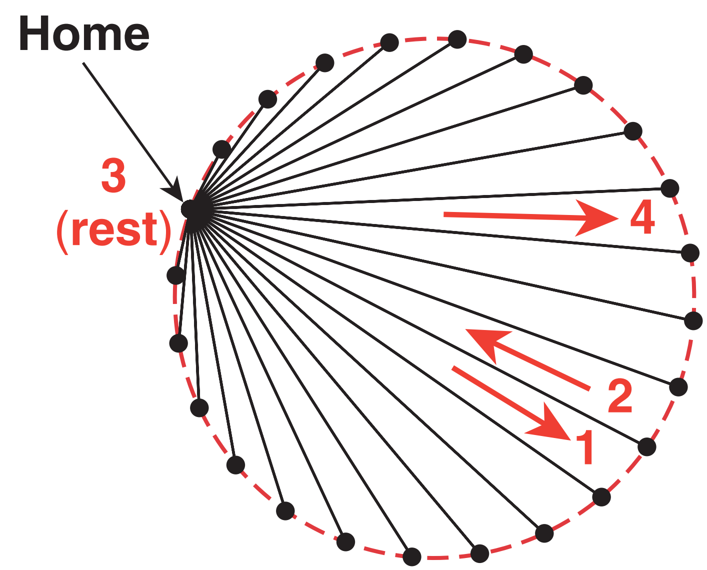

- Quick rotations followed by annealing rests ($\Delta t \geq 20$ min)
- The change is sufficiently small to allow determination of the low-mode number $Y_{\ell m}$ components.

E13440

The similarity between relaxed bright rings at all rotations indicates the primary influence is external to the target

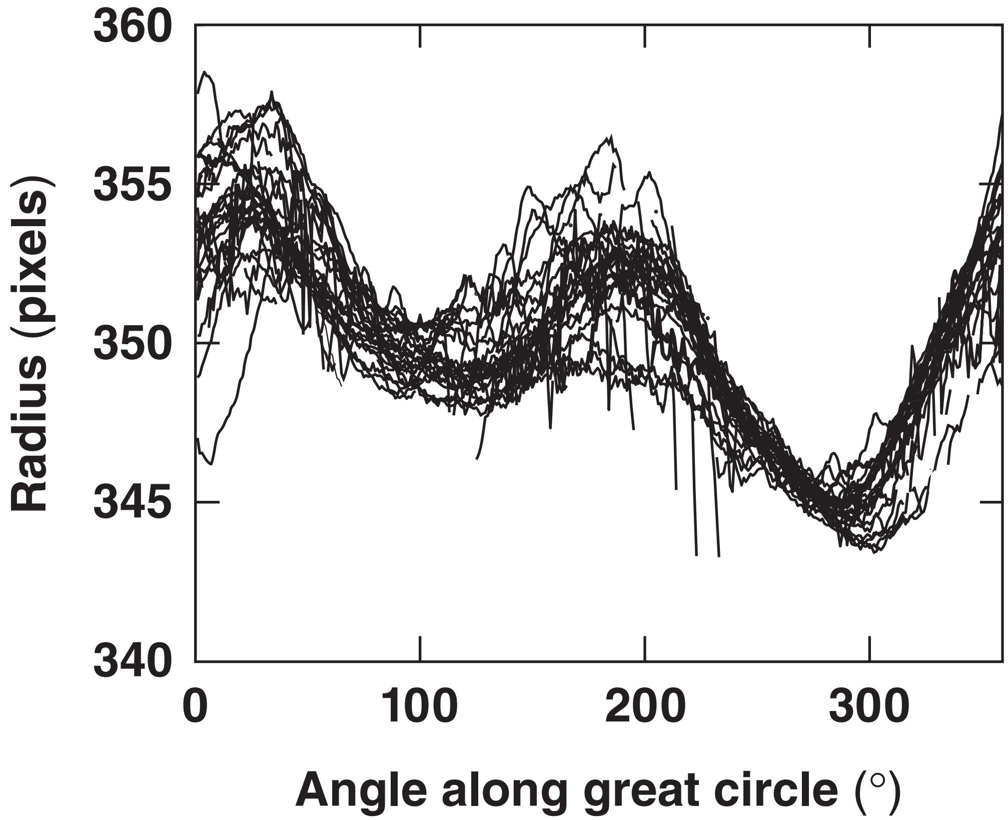

- Images taken after a 25 min rest at many rotation angles.
- Ice layer relaxes to a similar orientation with respect to the external layering-sphere geometry.
- Target shell thickness and uniformity are not a *primary* influence on layer uniformity.

E13438

Three-dimensional characterization is now standard procedure for LLE cryogenic targets

UR LLE

- Automated shadowgraphic analysis and 3-D characterization
  - bright ring identified to ~0.1 pixel (0.12 μm)
- 3-D characterization yields more detailed information on ice layer roughness and asymmetries

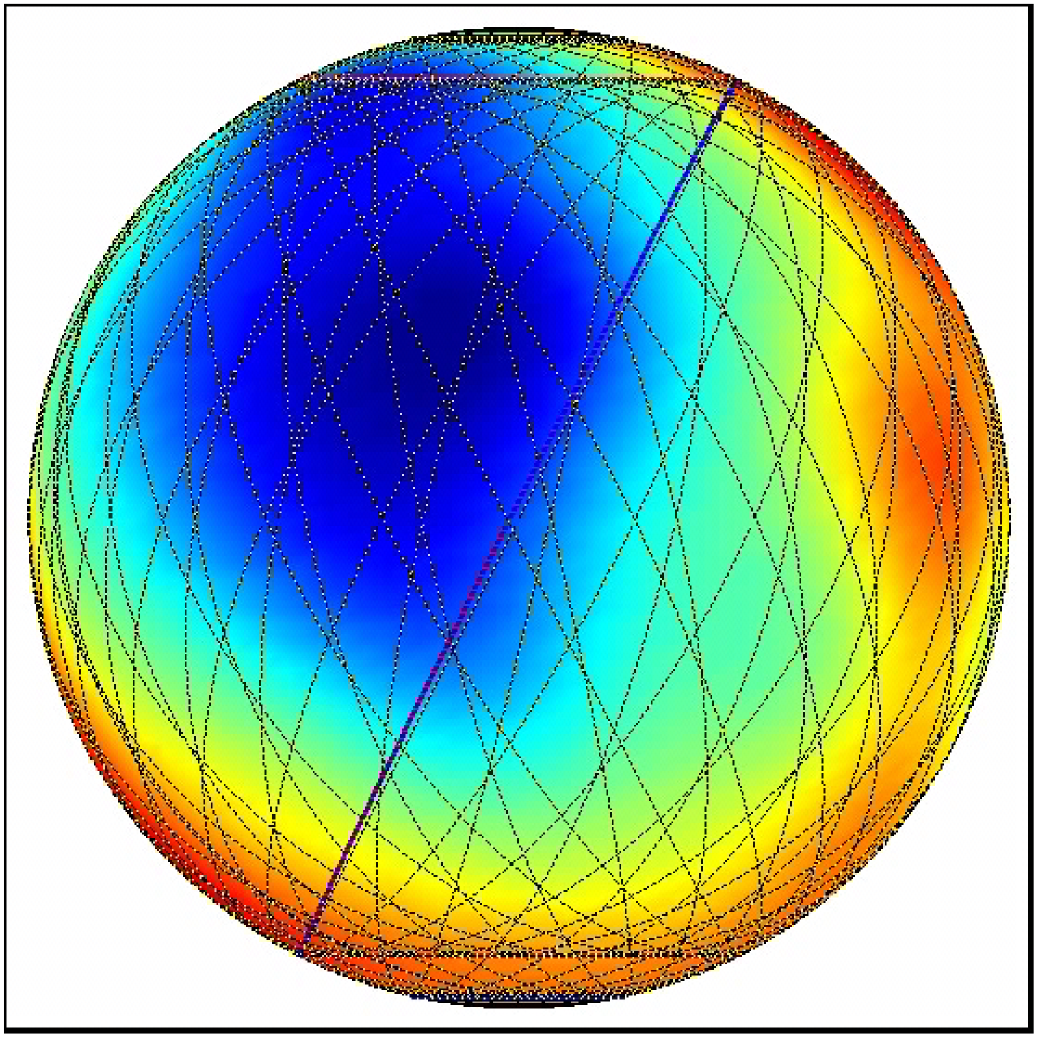

E13444

There are several possible sources of nonuniformity external to the target

- Layering sphere geometry
  - breaks in spherical geometry due to windows and keyhole
  - imperfect thermal contact between components
- Heating laser illumination
  - hot spots may occur at point of first bounce
  - sphere reflectivity not uniform due to damage from use on OMEGA
- Reduction of layering sphere nonuniformities will be needed to optimize ice layer quality

Uniformity of illumination of the inside of the layering sphere is not easily achieved

Half of the layering sphere

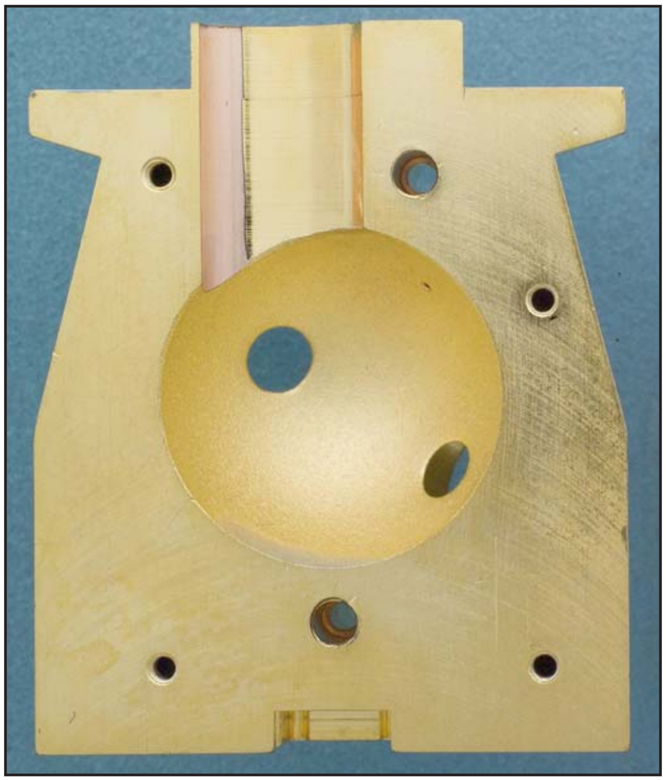

Typical commercial gold diffusers

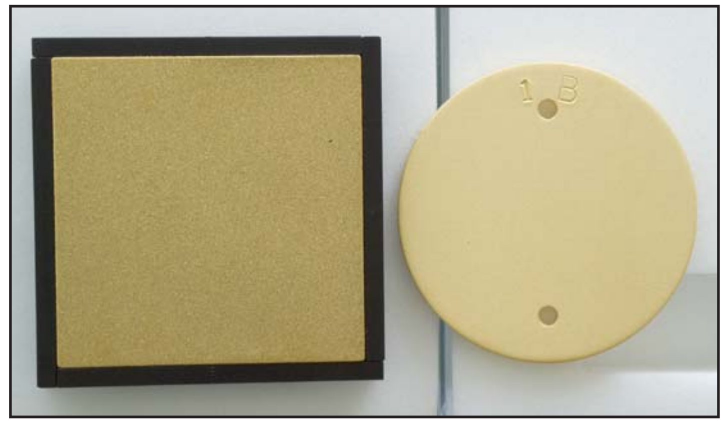

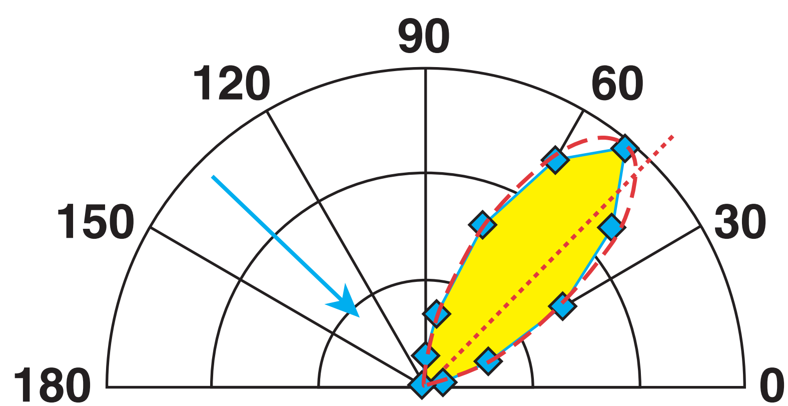

$\cos^9\theta \times \cos(\theta - \theta_0)$ distribution

E13521

Uniformity of illumination of the inside of the layering sphere is not easily achieved

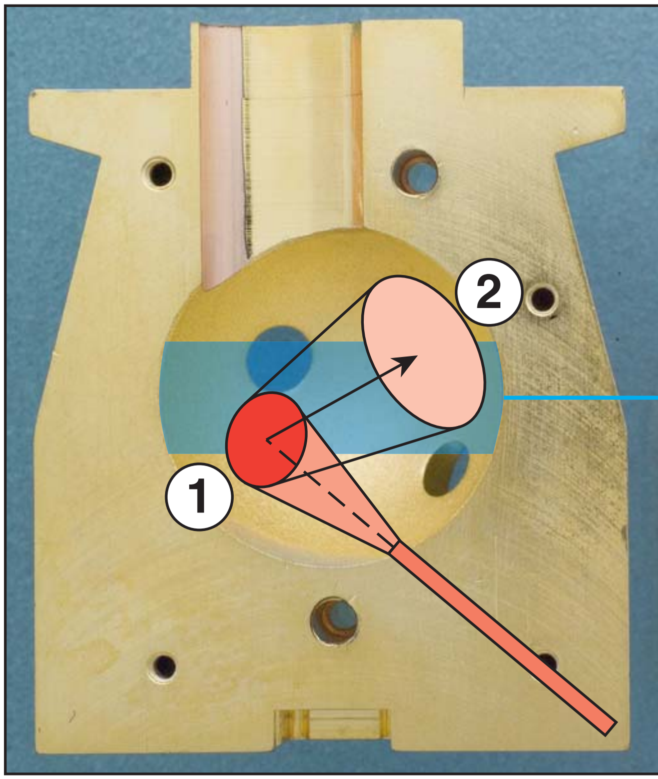

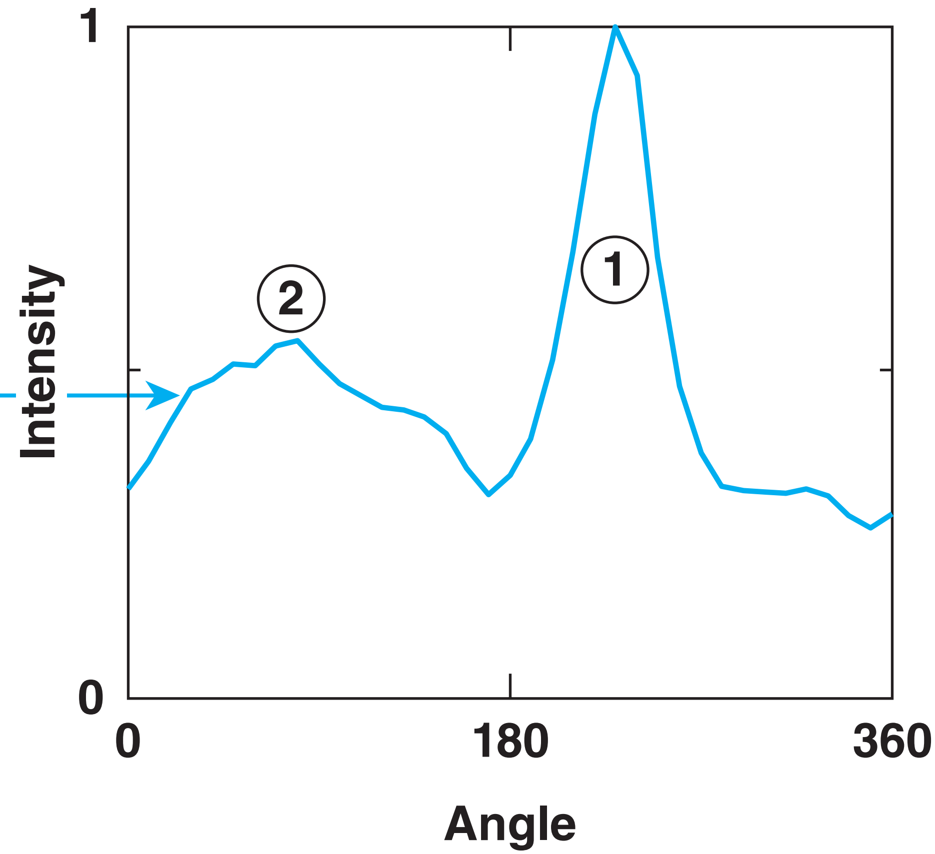

E13522

Uniformity of illumination of the inside of the layering sphere is not easily achieved

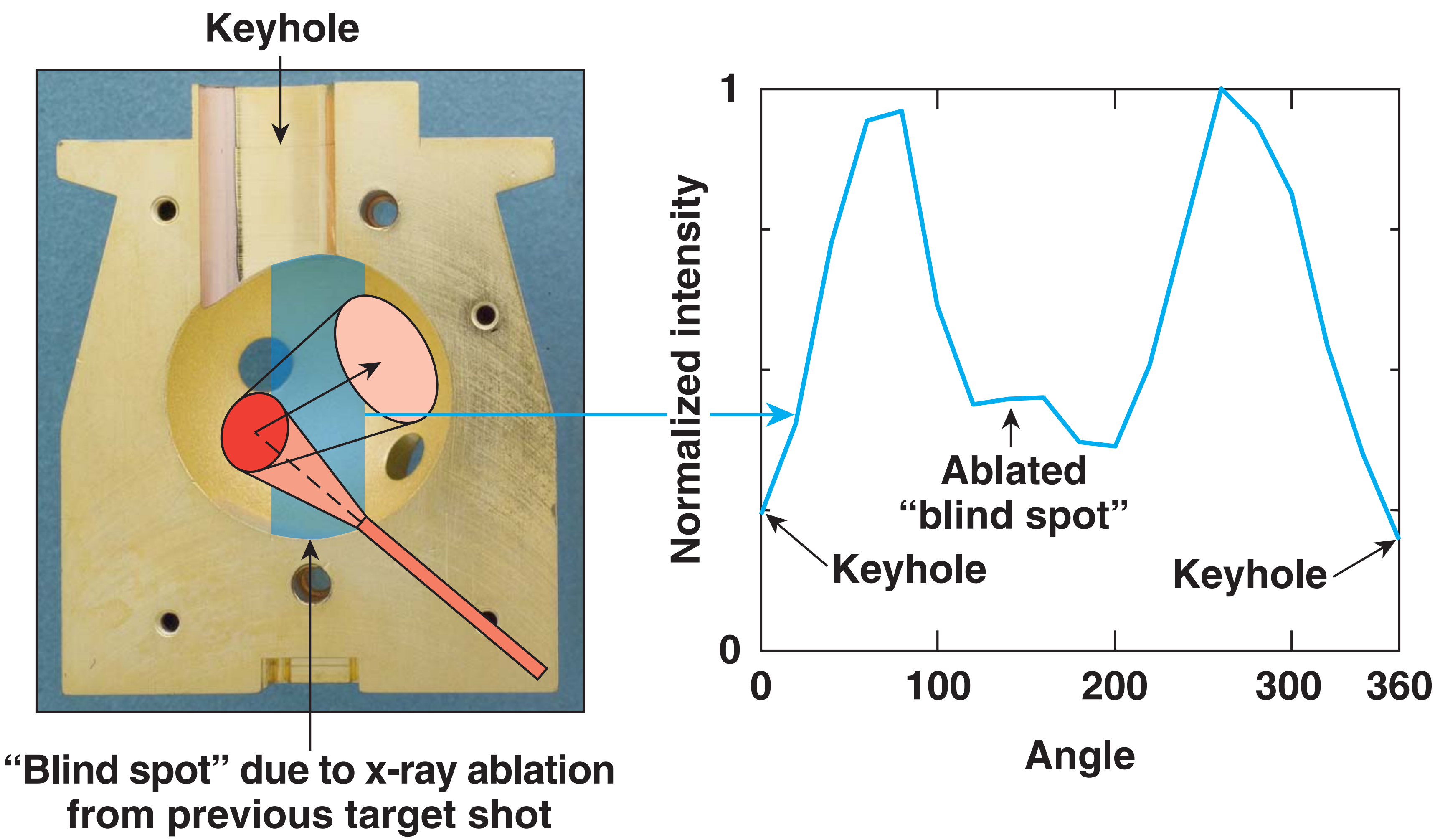

E13523

The D_2 ice index of refraction can be determined by simultaneously analyzing multiple rings

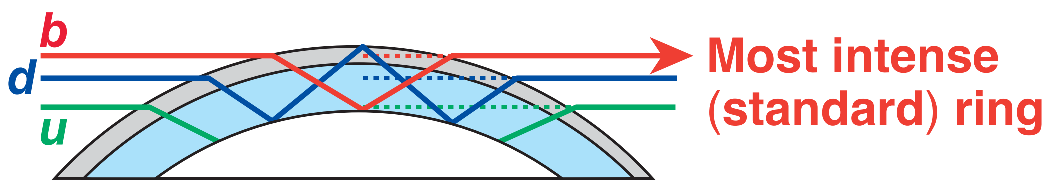

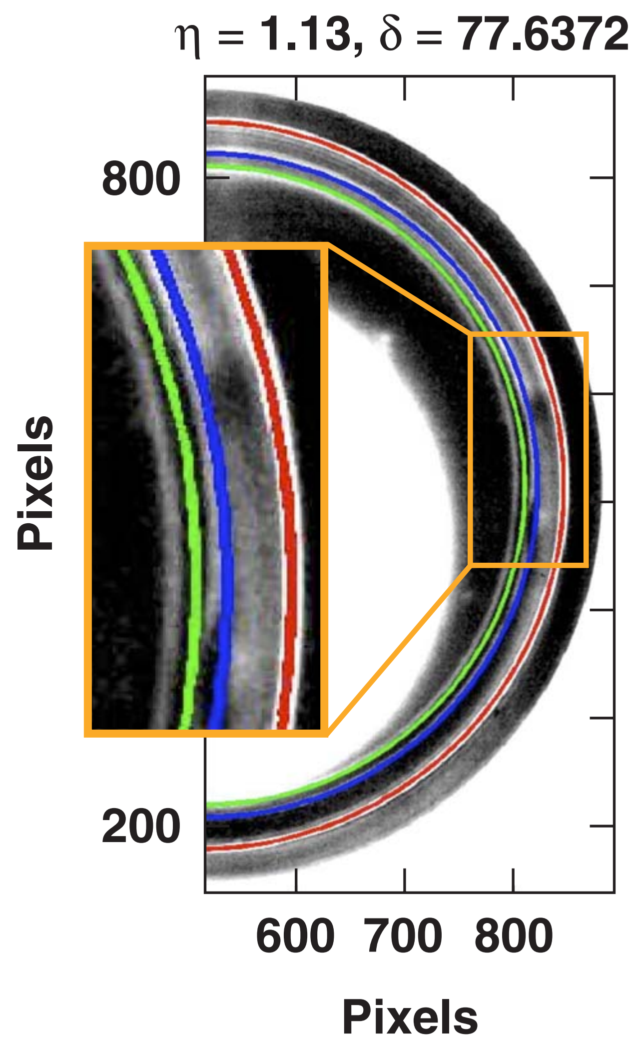

- Different rings depend differently on the ice layer thickness and index of refraction, η_{D_2}.
- The bright ring typically fits only to the ice thickness, assuming a fixed η_{D_2}.

Previous estimate: η_{D_2} = 1.13 doesn't produce a good match to all the rings.

Simultaneous fitting of multiple rings yields $\eta_{D_2} \approx 1.15$

- Fitting both ice thickness and η_{D_2} allows all rings to be matched.
- This results in a several percent change in estimated ice thickness.

η_{D_2} = 1.15 at λ = 644 nm produces a good match to all the rings.

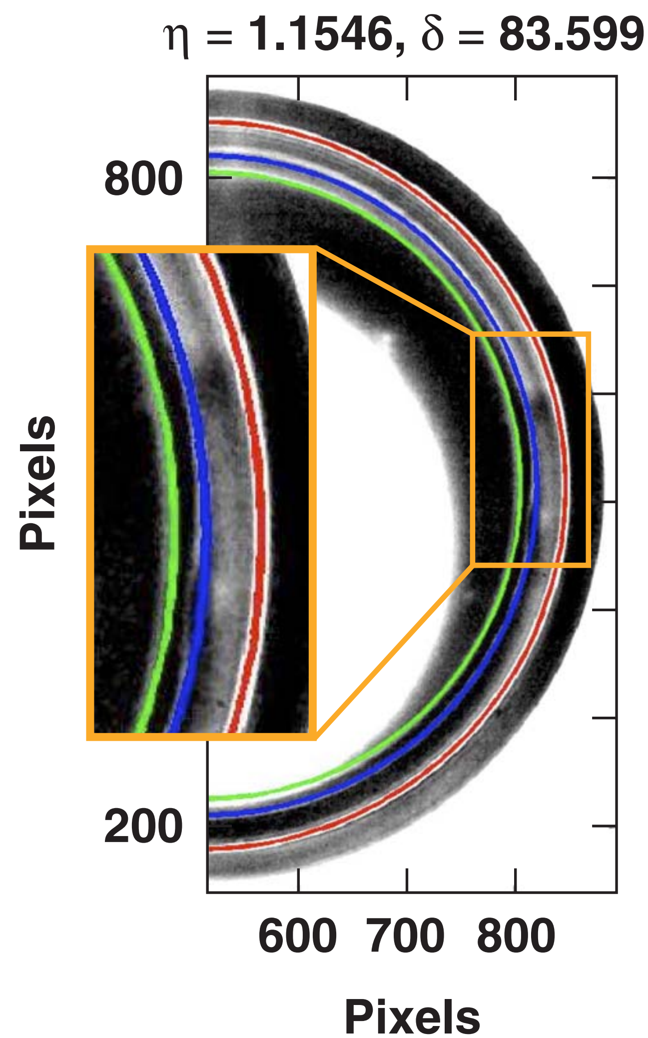

Summary/Conclusions

Optimization of layering geometry will be required to eliminate ice layer nonuniformities

UR LLE

- 3-D target characterization is standard operating procedure for OMEGA cryogenic targets.
- The D_2 ice index of refraction has been identified as ~1.15.
- Relayering was observed upon rotation of target inside the layering sphere.
  - time constants (~ 15 to 25 min near triple point)
- Target rotation and relayering studies show ice layer roughness dominated by external nonuniformities in the layering and heating geometry.

E13423